

# Trans-ethnic Meta-analysis and Functional Annotation Illuminates the Genetic Architecture of Fasting Glucose and Insulin

Ching-Ti Liu,<sup>1,84,\*</sup> Sridharan Raghavan,<sup>2,3,4,84</sup> Nisa Maruthur,<sup>5,6,7,84</sup> Edmond Kato Kabagambe,<sup>8,84</sup> Jaeyoung Hong,<sup>1</sup> Maggie C.Y. Ng,<sup>9,10</sup> Marie-France Hivert,<sup>11,12,13</sup> Yingchang Lu,<sup>14,15</sup> Ping An,<sup>16</sup> Amy R. Bentley,<sup>17</sup> Anne M. Drolet,<sup>18</sup> Kyle J. Gaulton,<sup>19</sup> Xiuqing Guo,<sup>20</sup> Loren L. Armstrong,<sup>21</sup> Marguerite R. Irvin,<sup>22</sup> Man Li,<sup>7</sup> Leonard Lipovich,<sup>18,23</sup> Denis V. Rybin,<sup>1</sup> Kent D. Taylor,<sup>20</sup> Charles Agyemang,<sup>24</sup> Nicholette D. Palmer,<sup>9,25</sup> Brian E. Cade,<sup>26</sup> Wei-Min Chen,<sup>27</sup> Marco Dauriz,<sup>28</sup> Joseph A.C. Delaney,<sup>29</sup> Todd L. Edwards,<sup>8</sup> Daniel S. Evans,<sup>30</sup> Michele K. Evans,<sup>31</sup> Leslie A. Lange,<sup>32</sup> Aaron Leong,<sup>2</sup> Jingmin Liu,<sup>33</sup> Yongmei Liu,<sup>34</sup> Uma Nayak,<sup>27</sup> Sanjay R. Patel,<sup>35</sup> Bianca C. Porneala,<sup>2</sup> Laura J. Rasmussen-Torvik,<sup>36</sup> Marieke B. Snijder,<sup>24</sup> Sarah C. Stallings,<sup>83</sup> Toshiko Tanaka,<sup>37</sup> Lisa R. Yanek,<sup>38</sup> Wei Zhao,<sup>39</sup> Diane M. Becker,<sup>38,40</sup> Lawrence F. Bielak,<sup>39</sup> Mary L. Biggs,<sup>41,42</sup> Erwin P. Bottinger,<sup>14</sup> Donald W. Bowden,<sup>9,10,25</sup> Guanjie Chen,<sup>17</sup> Adolfo Correa,<sup>43</sup> David J. Couper,<sup>44</sup> Dana C. Crawford,<sup>45</sup> Mary Cushman,<sup>46</sup> John D. Eicher,<sup>47,48</sup> Myriam Fornage,<sup>49</sup> Nora Franceschini,<sup>50</sup> Yi-Ping Fu,<sup>51</sup> Mark O. Goodarzi,<sup>52</sup> Omri Gottesman,<sup>14</sup> Kazuo Hara,<sup>14,53,54</sup> Tamara B. Harris,<sup>55</sup> Richard A. Jensen,<sup>42</sup> Andrew D. Johnson,<sup>48</sup> Min A. Jhun,<sup>39</sup> Andrew J. Karter,<sup>56</sup> Margaux F. Keller,<sup>57</sup> Abel N. Kho,<sup>21</sup> Jorge R. Kizer,<sup>58,59</sup> Ronald M. Krauss,<sup>60</sup> Carl D. Langefeld,<sup>61,62</sup> Xiaohui Li,<sup>20</sup>

(Author list continued on next page)

Knowledge of the genetic basis of the type 2 diabetes (T2D)-related quantitative traits fasting glucose (FG) and insulin (FI) in African ancestry (AA) individuals has been limited. In non-diabetic subjects of AA (n = 20,209) and European ancestry (EA; n = 57,292), we performed trans-ethnic (AA+EA) fine-mapping of 54 established EA FG or FI loci with detailed functional annotation, assessed their relevance in AA individuals, and sought previously undescribed loci through trans-ethnic (AA+EA) meta-analysis. We narrowed credible sets of variants driving association signals for 22/54 EA-associated loci; 18/22 credible sets overlapped with active islet-specific enhancers or transcription factor (TF) binding sites, and 21/22 contained at least one TF motif. Of the 54 EA-associated loci, 23 were shared between EA and AA. Replication with an additional 10,096 AA individuals identified two previously undescribed FI loci, chrX *FAM133A* (rs213676) and chr5 *PELO* (rs6450057). Trans-ethnic analyses with regulatory annotation illuminate the genetic architecture of glycemic traits and suggest gene regulation as a target to advance precision medicine for T2D. Our approach to utilize state-of-the-art functional annotation and implement trans-ethnic association analysis for discovery and fine-mapping offers a framework for further follow-up and characterization of GWAS signals of complex trait loci.

## Introduction

The global burden of type 2 diabetes (T2D [MIM: 125853]) is borne disproportionately by populations

with little genetic European ancestry (EA), especially African Americans.<sup>1</sup> Although environmental and behavioral factors account for a large portion of these observed race-ethnic disparities, genetic variation also contributes<sup>2,3</sup>

<sup>1</sup>Department of Biostatistics, School of Public Health, Boston University, Boston, MA 02118, USA; <sup>2</sup>Division of General Internal Medicine, Massachusetts General Hospital, Harvard Medical School, Boston, MA 02114, USA; <sup>3</sup>Department of Veterans Affairs Medical Center, Eastern Colorado Health Care System, Denver, CO 80220, USA; <sup>4</sup>Division of General Internal Medicine, Department of Medicine, University of Colorado School of Medicine, Denver, CO 80220, USA; <sup>5</sup>Division of General Internal Medicine, Johns Hopkins University School of Medicine, Baltimore, MD 21287, USA; <sup>6</sup>Welch Center for Prevention, Epidemiology, and Clinical Research, Johns Hopkins University, Baltimore, MD 21287, USA; <sup>7</sup>Department of Epidemiology, Johns Hopkins University Bloomberg School of Public Health, Baltimore, MD 21287, USA; <sup>8</sup>Division of Epidemiology, Department of Medicine, School of Medicine, Vanderbilt University Medical Center, Nashville, TN 37203, USA; <sup>9</sup>Center for Genomics and Personalized Medicine Research, Wake Forest University School of Medicine, Winston-Salem, NC 27157, USA; <sup>10</sup>Center for Diabetes Research, Wake Forest University School of Medicine, Winston-Salem, NC 27157, USA; <sup>11</sup>Department of Population Medicine, Harvard Pilgrim Health Care Institute, Harvard Medical School, Boston, MA 02215, USA; <sup>12</sup>Diabetes Unit, Massachusetts General Hospital, Boston, MA 02114, USA; <sup>13</sup>Department of Medicine, Université de Sherbrooke, Sherbrooke, QC J1G 0A2, Canada; <sup>14</sup>The Charles Bronfman Institute for Personalized Medicine, The Icahn School of Medicine at Mount Sinai, New York, NY 10029, USA; <sup>15</sup>The Genetics of Obesity and Related Metabolic Traits Program, The Icahn School of Medicine at Mount Sinai, New York, NY 10029, USA; <sup>16</sup>Division of Statistical Genomics, Department of Genetics, School of Medicine, Washington University, St Louis, MO 63108, USA; <sup>17</sup>Center for Research on Genomics and Global Health, National Human Genome Research Institute, NIH, Bethesda, MD 20892, USA; <sup>18</sup>Center for Molecular Medicine and Genetics, School of Medicine, Wayne State University, Detroit, MI 48201, USA; <sup>19</sup>Wellcome Trust Centre for Human Genetics, University of Oxford, Oxford OX3 7BN, UK; <sup>20</sup>Institute for Translational Genomics and Population Sciences, Department of Pediatrics, Los Angeles Biomedical Research Institute, Harbor-UCLA Medical Center, Torrance, CA 90502, USA; <sup>21</sup>Feinberg School of Medicine, Northwestern University, Chicago, IL 60611, USA; <sup>22</sup>Department of Epidemiology, School of Public Health, University of Alabama – Birmingham, Birmingham, AL 35294, USA; <sup>23</sup>Department of Neurology, School of Medicine, Wayne State University, Detroit, MI 48201, USA; <sup>24</sup>Department of Public Health, Academic Medical Center Amsterdam, Meibergdreef 15, 1105 AZ Amsterdam, the Netherlands; <sup>25</sup>Department of Biochemistry, Wake Forest University School of Medicine, Winston-Salem, NC 27157, USA; <sup>26</sup>Division of Sleep and Circadian Disorders, Brigham and

(Affiliations continued on next page)

Jingling Liang,<sup>63</sup> Simin Liu,<sup>64,65</sup> William L. Lowe, Jr.,<sup>21</sup> Thomas H. Mosley,<sup>66</sup> Kari E. North,<sup>50</sup> Jennifer A. Pacheco,<sup>21</sup> Patricia A. Peyser,<sup>39</sup> Alan L. Patrick,<sup>67</sup> Kenneth M. Rice,<sup>41</sup> Elizabeth Selvin,<sup>6,7</sup> Mario Sims,<sup>43</sup> Jennifer A. Smith,<sup>39</sup> Salman M. Tajuddin,<sup>31</sup> Dhananjay Vaidya,<sup>7,38</sup> Mary P. Wren,<sup>25</sup> Jie Yao,<sup>20</sup> Xiaofeng Zhu,<sup>63</sup> Julie T. Ziegler,<sup>61,62</sup> Joseph M. Zmuda,<sup>68</sup> Alan B. Zonderman,<sup>69</sup> Aeilko H. Zwinderman,<sup>24</sup> AAAG Consortium, CARE Consortium, COGENT-BP Consortium, eMERGE Consortium, MEDIA Consortium, Adebowale Adeyemo,<sup>17</sup> Eric Boerwinkle,<sup>49</sup> Luigi Ferrucci,<sup>37</sup> M. Geoffrey Hayes,<sup>21</sup> Sharon L.R. Kardia,<sup>39</sup> Iva Miljkovic,<sup>68</sup> James S. Pankow,<sup>70</sup> Charles N. Rotimi,<sup>17</sup> Michele M. Sale,<sup>27</sup> Lynne E. Wagenknecht,<sup>71</sup> Donna K. Arnett,<sup>72</sup> Yii-Der Ida Chen,<sup>20</sup> Michael A. Nalls,<sup>73</sup> MAGIC Consortium, Michael A. Province,<sup>16</sup> W.H. Linda Kao,<sup>7,85</sup> David S. Siscovick,<sup>29,42,74</sup> Bruce M. Psaty,<sup>29,42,75,76</sup> James G. Wilson,<sup>77</sup> Ruth J.F. Loos,<sup>14,15,78</sup> José Dupuis,<sup>1,47</sup> Stephen S. Rich,<sup>27</sup> Jose C. Florez,<sup>12,79,80,81</sup> Jerome I. Rotter,<sup>20</sup> Andrew P. Morris,<sup>19,82</sup> and James B. Meigs<sup>2,\*</sup>

but remains understudied in persons of mostly or all genetic African ancestry (AA).<sup>2–4</sup> A few studies have examined the association signals of EA-associated loci with levels of fasting glucose (FG) and insulin (FI) in ethnic minorities, but on a relatively small scale.<sup>5–7</sup> Genome-wide association studies (GWASs) with meta-analysis in EA populations have identified more than 50 loci associ-

ated with T2D-related quantitative traits (QTs), particularly levels of fasting glucose (FG) and insulin (FI).<sup>8</sup> Associated SNPs at these loci are common, with modest effect sizes.<sup>8–10</sup> At most SNPs the causal action remains unknown, because most lie in non-coding regions of the genome. Now, these have been annotated for regulatory function.<sup>11–14</sup> We collected a large sample of AA

Women's Hospital, Harvard Medical School, Boston, MA 02115, USA; <sup>27</sup>Center for Public Health Genomics, Department of Public Health Sciences, School of Medicine, University of Virginia, Charlottesville, VA 22908, USA; <sup>28</sup>Division of Endocrinology, Diabetes & Metabolism, Department of Medicine, University of Verona, 37126 Verona, Italy; <sup>29</sup>Department of Epidemiology, University of Washington, Seattle, WA 98195, USA; <sup>30</sup>California Pacific Medical Center Research Institute, San Francisco, CA 94107, USA; <sup>31</sup>Health Disparities Research Section, Laboratory of Epidemiology and Population Sciences, National Institute on Aging, NIH, Baltimore, MD 21224, USA; <sup>32</sup>Department of Genetics, University of North Carolina, Chapel Hill, NC 27607, USA; <sup>33</sup>Fred Hutchinson Cancer Research Center, Seattle, WA 98109, USA; <sup>34</sup>Center for Human Genetics, Division of Public Health Sciences, Wake Forest University School of Medicine, Winston-Salem, NC 27157, USA; <sup>35</sup>Department of Medicine, University of Pittsburgh, Pittsburgh, PA 15213, USA; <sup>36</sup>Department of Preventive Medicine, Feinberg School of Medicine, Northwestern University, Chicago, IL 60611, USA; <sup>37</sup>Translational Gerontology Branch, National Institute of Aging at Harbor Hospital, Baltimore, MD 21225, USA; <sup>38</sup>GeneSTAR Research Program, Division of General Internal Medicine, Department of Medicine, Johns Hopkins University, Baltimore, MD 21287, USA; <sup>39</sup>Department of Epidemiology, School of Public Health, University of Michigan, Ann Arbor, MI 48109, USA; <sup>40</sup>Department of Health Policy and Management, Johns Hopkins University Bloomberg School of Public Health, Baltimore, MD 21287, USA; <sup>41</sup>Department of Biostatistics, University of Washington, Seattle, WA 98195, USA; <sup>42</sup>Cardiovascular Health Research Unit, Department of Medicine, School of Medicine, University of Washington, Seattle, WA 98195, USA; <sup>43</sup>Department of Medicine, University of Mississippi Medical Center, Jackson, MS 39216, USA; <sup>44</sup>Collaborative Studies Coordinating Center, Department of Biostatistics, Gillings School of Global Public Health, University of North Carolina, Chapel Hill, NC 27514, USA; <sup>45</sup>Department of Epidemiology and Biostatistics, Institute for Computational Biology, Case Western Reserve University, Cleveland, OH 44106, USA; <sup>46</sup>Department of Medicine and Pathology, University of Vermont, College of Medicine, Burlington, VT 05405, USA; <sup>47</sup>National Heart, Lung, and Blood Institute's Framingham Heart Study, Framingham, MA 01702, USA; <sup>48</sup>Population Sciences Branch, Division of Intramural Research, National Heart, Lung, and Blood Institute, NIH, Framingham, MA 01702, USA; <sup>49</sup>Institute of Molecular Medicine and Human Genetics Center, University of Texas Health Science Center at Houston, Houston, TX 77030, USA; <sup>50</sup>Department of Epidemiology, University of North Carolina, Chapel Hill, NC 27514, USA; <sup>51</sup>Cardiovascular Epidemiology and Human Genomics Branch, National Heart, Lung, and Blood Institute, NIH, Framingham, MA 01702, USA; <sup>52</sup>Division of Endocrinology, Diabetes & Metabolism, Cedars-Sinai Medical Center, Los Angeles, CA 90048, USA; <sup>53</sup>Department of Diabetes and Metabolic Diseases, Graduate School of Medicine, The University of Tokyo, Tokyo 113-8655, Japan; <sup>54</sup>Department of Diabetes, Endocrinology, and Metabolism, Tokyo Medical University, Tokyo 163-0023, Japan; <sup>55</sup>Laboratory of Epidemiology and Population Sciences, NIH, Bethesda, MD 20892, USA; <sup>56</sup>Division of Research, Kaiser Permanente, Northern California Region, Oakland, CA 94612, USA; <sup>57</sup>Department of Genetics and Pharmacogenomics, Merck Research Laboratories, 33 Avenue Louis Pasteur, Boston, MA 02115, USA; <sup>58</sup>Department of Medicine, Albert Einstein College of Medicine, Montefiore Medical Center, Bronx, NY 10461, USA; <sup>59</sup>Department of Epidemiology and Population Health, Albert Einstein College of Medicine, Bronx, NY 10461, USA; <sup>60</sup>Children's Hospital Oakland Research Institute, Oakland, CA 94609, USA; <sup>61</sup>Center for Public Health Genomics, Wake Forest University School of Medicine, Winston-Salem, NC 27157, USA; <sup>62</sup>Department of Biostatistical Sciences, Wake Forest University School of Medicine, Winston-Salem, NC 27157, USA; <sup>63</sup>Department of Epidemiology and Biostatistics, Case Western Reserve University, Cleveland, OH 44106, USA; <sup>64</sup>Department of Epidemiology, Brown University, Providence, RI 02912, USA; <sup>65</sup>Department of Medicine, Brown University, Providence, RI 02903, USA; <sup>66</sup>Division of Geriatrics/Gerontology, Department of Medicine, University of Mississippi Medical Center, Jackson, MS 39216, USA; <sup>67</sup>Tobago Health Studies Office, Scarborough, Tobago, Trinidad and Tobago; <sup>68</sup>Department of Epidemiology, University of Pittsburgh, Pittsburgh, PA 15213, USA; <sup>69</sup>Behavioral Epidemiology Section, Laboratory of Epidemiology & Population Science, Intramural Research Program, National Institute on Aging, NIH, Baltimore, MD 21224, US; <sup>70</sup>Division of Epidemiology and Community Health, School of Public Health, University of Minnesota, Minneapolis, MN 55455, USA; <sup>71</sup>Division of Public Health Sciences, Wake Forest University School of Medicine, Winston-Salem, NC 27157, USA; <sup>72</sup>University of Kentucky College of Public Health, Lexington, KY 40563, USA; <sup>73</sup>Laboratory of Neurogenetics, National Institute on Aging, NIH, Bethesda, MD 20892, USA; <sup>74</sup>The New York Academy of Medicine, New York, NY 10029, USA; <sup>75</sup>Department of Health Services, University of Washington, Seattle, WA 98195, USA; <sup>76</sup>Group Health Research Institute, Group Health Cooperative, Seattle, WA 98101, USA; <sup>77</sup>Department of Physiology and Biophysics, University of Mississippi Medical Center, Jackson, MS 39216, USA; <sup>78</sup>The Mindich Child Health and Development Institute, The Icahn School of Medicine at Mount Sinai, New York, NY 10029, USA; <sup>79</sup>Center for Human Genetic Research, Massachusetts General Hospital, Boston, MA 02114, USA; <sup>80</sup>Programs in Metabolism and Medical & Population Genetics, Broad Institute, Cambridge, MA 02142, USA; <sup>81</sup>Department of Medicine, Harvard Medical School, Boston, MA 02115, USA; <sup>82</sup>Institute of Translational Medicine, Department of Biostatistics, University of Liverpool, Liverpool L69 3BX, UK; <sup>83</sup>Vanderbilt Institute for Clinical and Translational Research, Vanderbilt University Medical Center, Nashville, TN 37203, USA

<sup>84</sup>These authors contributed equally to this work

<sup>85</sup>Deceased

\*Correspondence: [ctliu@bu.edu](mailto:ctliu@bu.edu) (C.-T.L.), [jmeigs@partners.org](mailto:jmeigs@partners.org) (J.B.M.)

<http://dx.doi.org/10.1016/j.ajhg.2016.05.006>.

individuals for genetic study and, taking advantage of differences in linkage disequilibrium (LD) patterns across EA and AA, used a trans-ethnic analytic approach to improve mapping resolution<sup>15</sup> and narrow the number of potential causal SNPs at associated loci.<sup>15,16</sup> We then characterized predicted SNP function with detailed annotation information from diverse sources. We hypothesized that a trans-ethnic approach would identify SNPs with high likelihood of having regulatory, causal function, with results illuminating mechanisms underlying glycemic regulation in African Americans as well as whites of European ancestry.

We created the African American Glucose and Insulin Genetic Epidemiology (AAGILE) Consortium, with up to 20,209 AA individuals from 16 cohorts, to conduct a fixed effects meta-analysis of association summary statistics at 3.3 million (HapMap2) SNPs for levels of FG and body mass index (BMI)-adjusted FI. We then combined meta-analysis results from AAGILE with those from the EA Meta-Analyses of Glucose and Insulin-related traits Consortium (MAGIC,  $n = 57,292$ )<sup>10</sup> with three aims in mind: (1) conduct trans-ethnic fine-mapping of 54 T2D QT loci (36 FG, 16 FI, 2 associated with both FG and FI) identified from EA and combine fine-mapping with annotation resources including RegulomeDB, ENCYClopedia of DNA Elements (ENCODE), Islet Regulome, and Functional ANnotation of The mammalian genOME Consortium (FANTOM);<sup>11–14</sup> (2) assess the biologic relevance (allelic heterogeneity, transferability, population genetic selection, and consistency of association with T2D or insulin resistance traits) of the 54 EA FG and FI loci in AA individuals; and (3) identify additional FG and FI variants by combining association results from AAGILE and MAGIC using Meta-Analysis of TRans-ethnic Association Studies (MANTRA)<sup>15</sup> followed by de novo or in silico replication in additional AA samples ( $n$  up to 10,096) for 62 potential additional SNPs that met pre-specified significance levels from the trans-ethnic meta-analysis. The study design is illustrated in [Figure S1](#) and characteristics of each participating cohort are described in [Table S1](#).

## Material and Methods

### Research Participants

A total of 20,209 (for FG) and 17,871 (for FI) non-diabetic men and women of African ancestry (AA) from 16 cohorts participated in stage 1 ([Table S1](#)). Additionally, up to 10,096 (for FG) and 6,669 (for FI) non-diabetic individuals from 14 cohorts were included in a stage 2 replication analyses. Participants were excluded from this study if they had a diagnosis of T2D by a physician, were on any diabetes treatment, or had a FG concentration equal to or greater than 7 mmol/L. HbA1c levels were not used as diagnostic criteria. FG and FI GWAS data for 57,292 (FG) and 52,328 (FI) EA individuals were obtained from MAGIC.<sup>10</sup> Each participating study has obtained institutional review board approval and all subjects provided written informed consent.

### Genetic Variants

Genotyping was conducted in each cohort using commercially available genome-wide SNP arrays with quality control criteria for variants before imputation listed in [Table S1](#). In all stage 1 discovery analyses, imputation was performed to infer ungenotyped variants and fill in missing genotypes. We used phased haplotype data from the CEU and YRI HapMap phase 2 samples for the majority of contributing studies, using MACH<sup>17</sup> or IMPUTE2.<sup>18</sup> Variants with lower imputation quality scores ( $\text{MACH } r^2 < 0.30$  or IMPUTE2 information score  $< 0.40$ ) were excluded from further analyses. Approximately 3.3 million directly genotyped or imputed SNPs, including ~78,000 from the X chromosome, passed the quality control filters and were evaluated for association.

### Traits and Covariates

In all cohorts, fasting blood samples were obtained from participants after an overnight ( $\geq 8$  hr) fast. Detailed descriptions of study-specific FG and FI measurements are given in [Table S1](#). Analyses of untransformed levels of FG and natural logarithm-transformed FI were adjusted for age, age squared, sex, and principal components (PC) for ancestry. In addition, we adjusted FI levels for BMI to reduce confounding by obesity.<sup>10</sup> SNP-trait associations were tested using additive genetic models. Additional cohort-specific covariates (like study center for cohorts with multiple sites or relatedness for studies containing families) were included at the discretion of each cohort ([Table S1](#)).

### Overview of Study Design and Analysis Strategy

The overall study design is shown in [Figure S1](#). We first performed fixed-effect meta-analyses of FG and FI in AA samples. We then conducted trans-ethnic meta-analyses by combining the fixed-effect meta-analysis results from AAGILE with MAGIC. We fine-mapped FG and FI loci previously identified in EA by constructing 99% credible sets.<sup>15</sup> Second, we used results from the fixed-effect meta-analysis in AA to assess whether FG and FI loci identified in EA populations have genetic concordance or biological relevance in AA. Third, we carried forward 62 SNPs (not previously described to be associated with FG or FI in persons of EA) based on low fixed-effect meta-analysis  $p$  values in AA or high log-Bayes factor ( $\log(\text{BF})$ ) in the combined AA and EA trans-ethnic analysis for follow-up in additional non-diabetic samples of AA to identify additional FG and FI association signals. Specifically, the threshold for SNP promotion to replication was a fixed-effect meta-analysis  $p < 10^{-6}$  in AA samples, or  $p < 10^{-5}$  with  $\log(\text{BF}) > 5$  in MANTRA. Meta-analyses were performed at two different sites and summary statistics were crosschecked to ensure consistency of results.

### Meta-analysis of Samples from AAGILE and MAGIC Consortia

Each participating study from the AAGILE consortium performed a cohort-specific association analysis under an additive genetic model to test the genetic association of each genetic variant with FG and FI. The cohort-specific genome-wide association results were corrected with genomic control, unless  $\lambda_{\text{GC}} < 1$ , before meta-analyzing the GWAS results.<sup>17</sup> We then conducted a fixed-effects meta-analysis with inverse-variance weighting implemented in the program METAL to aggregate the cohort-specific association results.<sup>19</sup>

To leverage differential patterns of LD between common variants in EA and AA populations, we meta-analyzed GWAS results from AA in AAGILE and previously published EA results from MAGIC<sup>10</sup> using the Meta-ANalysis of Trans-ethnic Association Studies (MANTRA) software.<sup>15,20</sup> The results from MANTRA were used to fine-map the 54 loci (36 FG, 16 FI, 2 associated with both FG and FI) previously identified in EA samples and to prioritize variants for discovery of previously undescribed variants associated with FG and FI in AA samples.

### Construction of 99% Credible Sets

To improve fine-mapping resolution, we first constructed 99% credible sets for previously reported FG and FI loci identified in EA samples (36 FG, 16 FI, 2 associated with both FG and FI).<sup>8–10</sup> We identified the genomic region 250 kb upstream and 250 kb downstream of the lead SNP from the EA meta-analysis and defined  $BF_k$ , obtained from MANTRA analysis, as the Bayes factor for SNP  $k$ . We calculated the posterior probability that SNP  $k$  is functional or tagging an unobserved causal SNP by  $BF_k / \sum_i BF_i$ , where  $i$  indexes SNPs in the locus of interest. The 99% credible sets are the collection of the minimum number of variants providing a cumulative posterior probability greater or equal to 0.99 for representing the causal variant at a given locus.<sup>21</sup>

### Annotation of Credible Set SNPs

We focused our annotation analysis on loci that showed a 99% credible set reduction of at least 20% in the length of the genomic interval spanned by the variants in the credible set or in the number of variants included in the credible set (13 FG, 8 FI loci, and 1 locus for both FG and FI). When examining the distribution of credible set reduction across all 54 FG and FI loci, we noted that there appeared to be a natural break point between 20% and 12%, so we selected 20% reduction as a threshold defining loci with substantial reduction. At these loci, we classified SNPs in the credible set into two groups: one group with SNPs included in the 99% credible set from the trans-ethnic fine-mapping with MANTRA and a second group that included only SNPs that were included in the 99% credible set using EA samples (MAGIC) but were excluded from the trans-ethnic 99% credible set. For brevity, we henceforth refer to these categories of SNPs as the “narrowed sets” and “excluded sets,” respectively.

To compare functional annotation of the narrowed versus excluded credible sets, we annotated SNPs from the narrowed and excluded sets separately using the HaploReg tool that searches for dbSNP annotation (synonymous substitution, non-synonymous substitution, lying within an intron, 5' UTR, 3' UTR, or lncRNA, conservation in mammals, or having unknown position or function), genomic position, distance to the nearest named known protein-coding gene, eQTL data, and transcription factor motif, transcription factor binding site (TFBS), DNase hypersensitivity (DHS), and histone marks associated with promoters and enhancers derived from the ENCODE and Roadmap Epigenomics consortia.<sup>12</sup> We dichotomized the data from HaploReg for each SNP in the narrowed and excluded sets based on whether there was evidence of each specific annotation. To compare the narrow and excluded sets of SNPs for each trait, we performed a Fisher's exact test to assess differences in proportions of SNPs in each set with a specific annotation characteristic.

We visually examined overlap between trait association and regulatory annotation by plotting association statistics and regulatory data together. For each of the 22 loci with a reduction in the size

of at least 20% (either length of or the count of SNPs included in) of the 99% credible set after trans-ethnic analysis, we used RegulomeDB to generate a single numeric score summarizing the strength of regulatory data associated with each SNP in the locus (within 250 kb on either side of the index SNP for that locus from MAGIC).<sup>11</sup> In brief, RegulomeDB uses data from ENCODE and other published literature to annotate SNPs based on overlap with TFBS, TF motifs, DHS, eQTLs, and promoter histone marks and creates a score for each SNP ranging from 1 to 7, with 1 corresponding to the strongest degree of regulatory annotation, 6 corresponding to the weakest degree of regulatory annotation, and 7 representing no data available. We then used statistical software R to make regional association plots as described above using the  $\log(BF)$  for each SNP as the association statistic, with the color of each plotted SNP corresponding to its RegulomeDB score and the size of each plotted SNP corresponding to LD with the MAGIC index SNP in the YRI population. Finally, to visually examine overlap between the 99% credible regions at these 22 loci and regulatory data derived from pancreatic islets, we used the Islet Regulome Browser to generate plots with the same coordinates as represented in the regional plots and aligned the schematic representation of islet-derived regulatory annotation from the Islet Regulome Browser to the regional association plot.<sup>13</sup>

We performed additional annotation analyses for the narrowed set (from the trans-ethnic meta-analysis). The starting and ending chromosome position of the 99% credible region from the trans-ethnic analysis for each of the 22 loci with substantially reduced 99% credible sets were entered into the Islet Regulome Browser, and we cataloged the presence/absence of binding sites for five transcription factors (FOXA2, MAFB, NKX2.2, NKX6.1, PDX1) or the insulator protein CTCF, and histone marks associated with promoters, active enhancers, and inactive enhancers.<sup>11,13</sup> In addition to examining overlap between credible set SNPs and regulatory annotation, we also manually annotated the credible set intervals for the 22 loci with substantially reduced 99% credible sets. The genomic interval for each narrowed trans-ethnic credible set was examined in the UCSC Genome Browser, and we cataloged RNA expression, DHS sites, TFBS, and promoter and enhancer histone marks in cell types relevant to FG and FI, namely liver, pancreatic, adipose, and muscle.

### Genomic Annotation Enrichment Analysis

We tested for enrichment of chromatin state marks and TFBS using all variants in the trans-ethnic meta-analysis credible sets. We pooled chromatin states for promoter (TssA, TssFlnk) and enhancer (EnhA, EnhWk) elements for 93 cell types (after excluding cancer lines) from the Roadmap Epigenomics Consortium<sup>22</sup> and used TF binding data for 165 proteins from ENCODE<sup>23</sup> and the Islet Regulome.<sup>13</sup> For a given annotation, we calculated the cumulative posterior probability of annotated variants at each locus and then averaged these values across all loci. We then generated a null distribution for this procedure by randomly shuffling the probabilities among variants at each locus, recalculating the average probability for annotated variants, and repeating this procedure 1,000,000 times. We estimated fold-enrichment for each annotation by dividing the observed value by the permuted value averaged across all permutations. We then calculated a  $p$  value for the enrichment as the proportion of permutations for which the resulting value was greater than or equal to that observed. We applied a corrected significance threshold of 0.00019 (0.05/257 annotations).



## Interrogation of Transferability across Populations

We investigated the transferability to AA of EA FG- and FI-associated SNPs and loci. To evaluate SNP transferability, we tested in AA the association of index FG and FI SNPs from EA individuals in MAGIC<sup>8–10</sup> (i.e., EA FG or FI SNPs with  $p < 5 \times 10^{-8}$ ). We defined SNP transferability as an EA index SNP showing in AA an association that was statistically significant ( $p < 0.05$ ) and consistent in direction of effect as in the EA meta-analysis. To evaluate locus transferability, given differences in local LD structure across populations, we also interrogated the flanking  $\pm 250$  kb regions of the index SNP in AA to search for any SNPs with a smaller association  $p$  than the EA index SNP. For locus transferability, we used a Bonferroni corrected  $p$  to determine the significance for each locus by adjusting for the effective number of independent tests within that locus, using the Li and Ji approach.<sup>24</sup>

## Conditional Analysis of Signals with Significant SNP Associations in AA

We performed approximate conditional association analyses at loci with significant QT associations in AAGILE in order to test whether the associated AAGILE SNP was the same association signal as the MAGIC SNP. We used genome-wide complex trait analysis (GCTA)<sup>25</sup> for this analysis, because it allows approximate conditional analyses in results from meta-analysis without the need for individual cohort data to conduct the tests. GCTA approximated the variance-covariance matrix of genotype using estimated allele frequency from the meta-analysis results and LD between SNPs from a reference sample. We calculated the association of the AA best SNP conditional on the EA index SNP within the same locus in AA samples.

## Concordance Analysis across Ancestry Groups

For this analysis, we considered SNPs that passed QC and had a MAF  $> 1\%$  in both EA- and AA-specific meta-analyses. We further excluded (1) EA-associated FG or FI loci, defined as those lying 500 kb upstream or downstream of previously reported SNPs for each loci as described,<sup>16</sup> and (2) AT/GC SNPs to avoid the potential bias introduced by the strand misalignment between EA- and AA-specific meta-analysis. We then classified all the remaining SNPs into categories based on the association  $p$  value in the MAGIC EA samples:  $p \leq 0.01$ ,  $0.01 < p \leq 0.5$ , and  $0.5 < p \leq 1$ . For the SNPs within each category, we then selected a set of independent SNPs by identifying the most significant SNP, omitting the SNPs within 500 kb region apart from the most significant SNP, and then repeating this process until there were no more SNPs left. We then determined the direction of effect for the EA trait-raising allele between EA and AA samples and we calculated the proportion of these selected SNPs that share the same direction of effect. To determine the significance of the excess in concordance (with 50% expected), we then conducted one-sided binomial tests.

## Population Differentiation and Natural Selection at QT Loci

We applied several approaches to evaluate population differentiation and natural selection at index FG or FI SNPs, using the trait-raising allele in EA as the risk allele. First, we compared the risk-allele frequencies in EA versus AA by calculating the absolute value difference between the risk-allele frequency in EA and the risk-allele frequency in AA for each index SNP. Second, we used Wright's fixation index<sup>26</sup> ( $F_{st}$ ) to measure the degree of the popu-

lation differentiation due to genetic drift and reflected by the divergent allele frequencies. A value of  $F_{st}$  lying in range of 0 to 0.05 indicates little genetic differentiation; a value 0.05 to 0.15, moderate differentiation; and a value greater than 0.15, greater population differentiation.<sup>27,28</sup> We calculated  $F_{st}$  using risk-allele frequencies obtained from AAGILE cohorts for AAs and from MAGIC<sup>8–10</sup> for EAs. We also calculated the  $F_{st}$  using CEU and YRI HapMap2 data from two samples of equal size to ensure that the imbalance in sample size of our EA and AA samples does not obscure the population differentiation at any locus. Third, we used Haplotter<sup>29</sup> to calculate the integrated haplotype score (iHS) in HapMap2 data to measure the amount of extended haplotype homozygosity and hence the evidence of recent positive selection at the index SNP. Fourth, we compared the effect alleles from the index SNP of each locus against the human genome to determine whether it was the major or minor allele using the UCSC Genome Browser GRCh37/hg19 version, produced by the Genome Reference Consortium in 2009.<sup>30</sup>

## Associations of QT Loci with T2D and Insulin Resistance-Related Traits in AA Individuals

As described below, we assembled new African ancestry cohort data sources for triglycerides and initiated collaborations with new and existing consortia for body mass index (BMI), waist-to-hip ratio adjusted for BMI (WHRadjBMI), systolic and diastolic blood pressure, hypertension (HTN), and low-density and high-density lipoprotein cholesterol (LDL-C and HDL-C) to investigate the association of T2D QT SNPs with T2D and insulin resistance-related traits (BMI, WHRadjBMI, HTN, LDL-C, HDL-C, and triglycerides) in AA individuals. Specifically, we investigated the association of 25 SNPs, including 24 most associated SNPs (14 FG, 9 FI, and 1 SNP, rs780094, associated with both FG and FI) residing in the regions demonstrating locus transferability in AA and 1 previously undescribed FI SNP (rs6450057). We also tested the association of the FI SNP on chromosome X, rs213676, with lipid traits (the only traits available for chromosome X). HapMap2-imputed GWAS meta-analysis summary statistics for 25 SNPs were obtained from the Meta-analysis of T2D in African Americans (MEDIA) consortium for T2D<sup>31</sup> (n up to 23,818), the African Ancestry Anthropometry Genetics Consortium (AAAGC) for BMI<sup>32</sup> (n up to 39,141) and WHRadjBMI<sup>32,33</sup> (n up to 19,049), and the Continental Origins and Genetic Epidemiology Network (COGENT) for HTN and blood pressure<sup>34</sup> (n up to 29,828). HapMap-imputed GWAS meta-analysis summary statistics for 26 SNPs were obtained from the Candidate gene Association Resource (CARE) consortium for LDL-C and HDL-C<sup>35</sup> (n up to 8,090) and the Electronic Medical Records and Genomics Network (eMERGE) for triglycerides<sup>36</sup> (n up to 2,838). SNPs with  $p < 0.05$  and same direction of effect (i.e., FG/FI-increasing alleles associated with T2D or higher levels of the quantitative insulin-resistance traits, except for HDL-C where FG/FI-increasing alleles were expected to be associated with lower HDL-C) were considered significant.

## Discovery and Replication of Previously Undescribed FG and FI SNPs in AA

For identification of additional FG- and FI-associated loci in AA, we took a two-stage (discovery followed by replication) approach (Figure S1). In the discovery stage, we used fixed-effect meta-analysis results in AA and the trans-ethnic meta-analysis (MANTRA) results as described in the [Meta-analysis of Samples from AAGILE and MAGIC Consortia](#) section. We identified 62 variants, not

previously reported to be associated with FG or FI in any ancestry, classified into three tiers of decreasing restrictiveness based on low fixed-effect meta-analysis  $p$  values in AA or high trans-ethnic meta-analysis (MANTRA)  $\log(\text{BF})$  in the combined AA and EA results, for follow-up in 10,096 additional AA samples from 16 additional, independent cohorts (Table S1). Identified variants were classified into three tiers to take forward to the replication stage. Tier 1 was variants with a fixed-effect meta-analysis  $p < 10^{-6}$  in AA samples, or  $p < 10^{-5}$  with  $\log(\text{BF}) > 5$  in MANTRA; tier 2 was variants with  $\log(\text{BF}) > 4$  and fixed-effect  $p < 10^{-5}$ ; and tier 3 was variants with  $\log(\text{BF}) > 4$  or fixed-effect  $p < 10^{-5}$  (Figure S1).

The 16 additional independent replication cohorts are listed in Table S1. For replication, we sought either in silico look-ups of the 62 SNPs that met criteria for one of the three tiers from the discovery stage in the cohorts with extant genotyping array data or conducted de novo genotyping for SNPs in tier 1 in additional cohorts with DNA and trait levels. Each participating replication cohort implemented the same model used for discovery analyses to evaluate associations between SNPs and traits. First we compared discovery and replication results for significance and direction of effect. Then we meta-analyzed the discovery and replication stage results to obtain a combined, fixed effect inverse variance estimate for each of the 62 SNPs. Genome-wide statistical significance was set at  $p \leq 5 \times 10^{-8}$ , and associations were considered to be previously undescribed if they were not in LD ( $r^2 < 0.3$  or not within 500 kb of a previously reported glycemia-associated SNP).

Finally, we performed a trans-ethnic meta-analysis in MANTRA combining fixed effects estimates from the AAGILE discovery and replication combined meta-analysis with published EA results from MAGIC to get a trans-ethnic total effect size using all available data for 62 SNPs. We considered an association to have reached genome-wide significance if the  $p \leq 5 \times 10^{-8}$  in fixed-effect meta-analysis or  $\log(\text{BF})$  from MANTRA was greater than 6, and we considered the association to be previously undescribed if the variants were not in LD ( $r^2 < 0.3$ ) or not within 500 kb of a SNP previously reported to be associated with FG or FI.

## Results

### Trans-ethnic Fine-Mapping and Annotation of Glycemic QT Loci Established in EA Populations

To fine-map 54 loci previously associated with FG or FI in EA,<sup>8–10</sup> we constructed 99% credible sets, the smallest set of SNPs that accounts for 99% of the posterior probability of containing the causal variant at the locus, using meta-analysis results only from MAGIC EA samples and trans-ethnic meta-analysis results from both MAGIC EA samples and AAGILE AA samples (Table S2). Reflecting increased sample size and differences in LD structure between ancestry groups, trans-ethnic meta-analyses yielded more than 20% reduction in either the number of SNPs or the genomic interval spanned by the SNPs in credible sets for 22/54 loci (13 FG, 8 FI, and 1 associated with both FG and FI; Table 1 and Figures S2 and S3) while we also observed some loci with substantially enlarged credible sets. For 4 of these 22 loci (*GCK* [MIM: 138079] and *ADCY5* [MIM: 600293] for FG, *PPP1R3B* [MIM: 610541] for FI, and *GCKR* [MIM: 600842] for both) with a >20% reduction in the credible set, the credible set included a sin-

gle SNP. We observed the greatest reduction (95%) in the number of SNPs in the credible set at the *FOXA2* locus, where the genomic width of the credible set was also greatly reduced (from ~46 kb to ~4 kb; 92% reduction), and the extent of LD surrounding the index SNP was less in AA than EA (Figure 1). The narrowed trans-ethnic CSs contained previously described functional variants at several loci, including the coding SNP rs1801282 (GenBank: NC\_000003.12; g.12351626C>G [p.Pro12Ala]) in *PPARG* (MIM: 601487)<sup>37</sup> and rs7903146 in *TCF7L2* (MIM: 602228), which has been shown to overlap an islet enhancer and modify enhancer activity.<sup>38</sup> In contrast, the coding SNP rs1260326 at the *GCKR* locus, presumed to be causal based on prior studies,<sup>39,40</sup> was excluded from the 99% credible set. With the exception of non-synonymous variants at *DPYSL5* (MIM: 608383), *COBLL1* (MIM: 610318)-*GRB14* (MIM: 601524), and *PPARG* (Table 2), the greatly reduced credible sets mapped predominantly to non-coding sequences.

At 22 loci with a >20% reduction in the credible set, we compared functional annotations of SNPs in the trans-ethnically generated credible sets (“narrowed” set) to those of SNPs excluded from the EA-only credible sets (“excluded” set) using HaploReg annotation.<sup>12</sup> For the narrowed set of nine FI loci, the SNP annotation from dbSNP indicated only a reduction in intronic SNPs and an increase in unknown function SNPs compared to the excluded set (Table S3). However, regulatory annotation data showed that the narrowed set of nine FI loci was enriched for enhancer-associated chromatin marks and eQTLs when compared to the excluded set (76.3% versus 66.0%,  $p = 0.004$  for enhancer marks; 39.4% versus 28.5%,  $p = 0.002$  for eQTLs [Table S3]). At the 14 FG loci, we observed an enrichment of SNPs in 3' UTR of genes, but no enrichment of regulatory annotations in the narrow set compared to the excluded set (Table S4). Table S5 provides annotation information from HaploReg for each SNP in these 22 derived credible sets, and the Supplemental Note and Table S6 show results from more extensive annotation from publicly available regulatory data. As an example, manual annotation of the *FOXA2* locus shows that the top SNP lies just upstream of an lncRNA, LINC00261, with evidence for expression in liver and pancreas and overlapping numerous TFBSs in liver cell lines (Supplemental Note). This and prior evidence that this lncRNA can regulate *FOXA2* expression<sup>41</sup> implicate the lncRNA as a possible causal transcript at this locus.

To more specifically examine whether variants at the 22 loci with greatly narrowed credible sets were enriched for individual TFBS or cell-type-specific chromatin marks, we employed a permutation test. We observed significant enrichment ( $p < 1.9 \times 10^{-4}$ ) for FG loci at binding sites for MAFB ( $p = 2 \times 10^{-6}$ ), NKX2-2 ( $p = 2 \times 10^{-6}$ ), *FOXA2* ( $p = 1.6 \times 10^{-5}$ ), and PDX1 ( $p = 1.0 \times 10^{-4}$ ) as well as for chromatin marks in pancreatic islets ( $p = 1.2 \times 10^{-4}$ ) (Figure 2A, Table S7). Among FI loci, we observed nominally significant enrichment for chromatin marks in

**Table 1. 22 EA-Associated Type 2 Diabetes Quantitative Traits Loci with Substantially Reduced 99% Credible Sets Based on Trans-ethnic Fine Mapping**

Locus <sup>a</sup>	Chr	99% Credible Set: European Ancestry Only		99% Credible Set: Trans-ethnic		99% Credible Set Reduction	
		# SNPs <sup>b</sup>	Range <sup>c</sup> (bp)	# SNPs <sup>b</sup>	Range <sup>c</sup> (bp)	% SNPs <sup>d</sup>	% Range <sup>e</sup>
<b>Fasting Glucose-Associated Loci</b>							
<i>FOXA2</i>	20	40	46,365	2	3,872	95.0	91.6
<i>GCK</i>	7	7	25,107	1	1	85.7	100.0
<i>KL</i>	13	696	496,262	147	492,550	78.9	0.7
<i>ADCY5</i>	3	4	31,042	1	1	75.0	100.0
<i>GCKR</i>	2	2	11,663	1	1	50.0	100.0
<i>PROX1</i>	1	11	18,286	6	13,550	45.5	25.9
<i>DPYSL5</i>	2	87	294,065	50	269,667	42.5	-8.3
<i>IGF2BP2</i>	3	64	317,522	38	355,236	40.6	-11.9
<i>CDKN2B-ANRIL</i>	9	7	5,914	5	4,515	28.6	23.7
<i>ADRA2A</i>	10	33	68,716	26	68,110	21.2	0.9
<i>TCF7L2</i>	10	5	36,312	4	15,268	20.0	58.0
<i>FADS1</i>	11	20	58,394	16	57,823	20.0	1.0
<i>DGKB-TMEM195</i>	7	11	143,605	10	2,182	9.1	98.5
<i>CRY2</i>	11	10	57,088	11	14,850	-10.0	74.0
<b>Fasting Insulin-Associated Loci</b>							
<i>ARL15</i>	5	319	498,585	22	33,535	93.1	93.3
<i>PPP1R3B</i>	8	8	9,510	1	1	87.5	100.0
<i>COBLL1-GRB14</i>	2	14	51,528	3	11,540	78.6	77.6
<i>IRS1</i>	2	43	137,640	13	68,951	69.8	49.9
<i>GCKR</i>	2	3	11,663	1	1	66.7	100.0
<i>FAM13A</i>	4	43	243,374	21	243,374	51.2	0.0
<i>ANKRD55-MAP3K1</i>	5	417	497,027	218	487,103	47.7	2.0
<i>UHRF1BP1</i>	6	13	217,136	9	136,609	30.8	37.1
<i>PPARG</i>	3	14	60,448	11	56,618	21.4	6.3

The 22 EA-associated T2D QT loci include 13 fasting glucose, 8 fasting insulin, and 1 associated with both. Substantial reduction is defined as greater than 20% reduction in its genomic length or the number of SNPs.

<sup>a</sup>For ease of comparison to previous studies, the loci are named based on the historically identified nearest protein-coding gene or genes to the index SNP in European ancestry.

<sup>b</sup># SNPs is the number of SNPs included in the 99% credible set.

<sup>c</sup>Range is defined as the maximum genomic distance based on hg18 among the SNPs included in the 99% credible set.

<sup>d</sup>%SNPs is (the number of SNPs in the EA-based 99% credible set – the number of SNPs in the trans-ethnic analysis-based 99% credible set)/the number of SNPs in the EA-based 99% credible set.

<sup>e</sup>%Range is (the range of the EA-based 99% credible set – the range of the trans-ethnic analysis-based 99% credible set)/the range of the EA-based 99% credible set.

adipose cells ( $p = 0.048$ ) and for several TFBSs such as MAFK ( $p = 0.0038$ ) and RXRA ( $p = 0.0071$ ) (Figure 2A, Table S7).

We incorporated information from RegulomeDB and the Islet Regulome Browser<sup>11,13</sup> to better visualize the relationship between trait association and regulatory annotation at the 22 loci with >20% reduction in the 99% credible sets. Of the 14 FG loci, seven (*CRY2* [MIM: 603732], *DPYSL5*, *FADS1* [MIM: 606148], *FOXA2*, *GCKR*, *IGF2BP2* [MIM: 608289], and *KL* [MIM: 604824]) contained a SNP with a RegulomeDB score  $\leq 3$ , consistent with moderate

evidence for regulatory function (Figure S4). At four of these seven loci (*CRY2*, *FADS1*, *FOXA2*, and *GCKR*), the same SNP with strong regulatory annotation also had genome-wide significant evidence of association in the trans-ethnic meta-analysis ( $\log(\text{BF}) > 6$ ) (Figures 2B, 2C, and S4). Similarly, of the nine FI loci with reduced credible set size, six of the credible regions (*ANKRD55* [MIM: 615189]-*MAP3K1* [MIM: 600982], *ARL15*, *FAM13A* [MIM: 613299], *GCKR*, *PPARG*, and *UHRF1BP1*) contained a SNP with a RegulomeDB score  $\leq 3$ , and at three of these loci (*GCKR*, *PPARG*, and *UHRF1BP1*), the SNP with strong

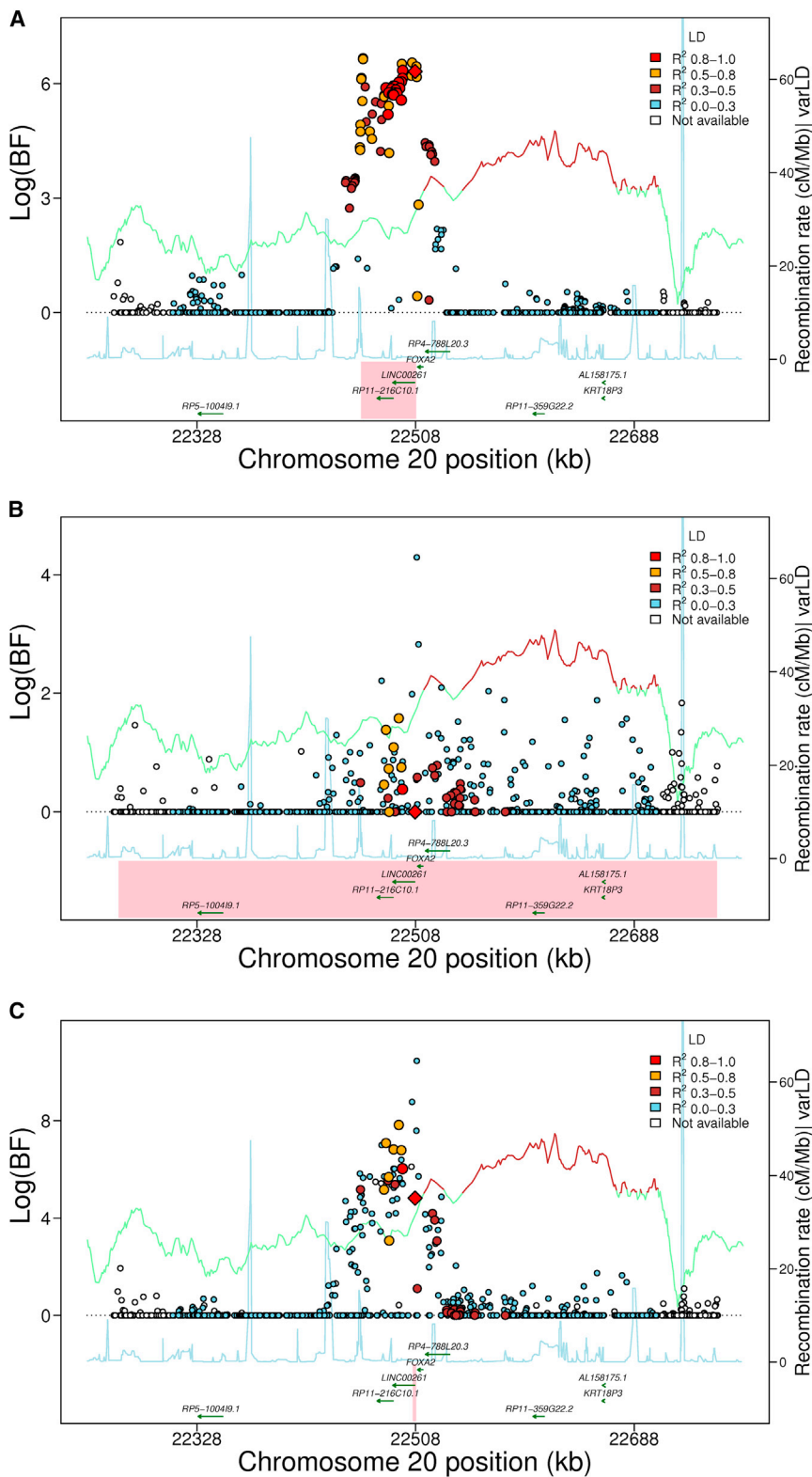


**Figure 1. Trans-ethnic Analysis of Glycemic Quantitative Loci Provides Narrowed Intervals Spanned by the 99% Credible Set**

Data are 500 kb regional association plots for fasting glucose at *FOXA2*, centered at the index SNP identified from European ancestry (EA) samples. The x axis denotes genomic position and the y axis denotes the log (BF), recombination rate, and varLD information<sup>61</sup> (a measure to quantify LD variation differences comparing populations). The red diamond data point represents the index SNP within the region previously reported from EA samples. The color of each data point indicates its LD value ( $r^2$ ) with the index SNP based on HapMap2 (YRI for AA results and CEU for EA results): white,  $r^2$  not available; blue,  $r^2 = 0.0-0.2$ ; brown,  $r^2 = 0.2-0.5$ ; orange,  $r^2 = 0.5-0.8$ ; red,  $r^2 = 0.8-1.0$ . The blue line represents the recombination rate. The green line shows the varLD score at each SNP and is highlighted with dark brown if the varLD score is  $>95^{\text{th}}$  percentile of the genome-wide varLD score, comparing LD information between YRI and CEU HapMap2 samples.<sup>61</sup> The interval spanned by the 99% credible set is highlighted in pink.

(A) Association results for fasting glucose in the *FOXA2* region in EA individuals. The 99% credible set contains 40 SNPs that span an interval of 46,365 bp.

(B) Association results for fasting glucose in the *FOXA2* region in AA individuals. The association signal is weaker than in EA samples, leading to a wider interval spanned by the 99% credible set.

(C) Association results for fasting glucose in the *FOXA2* region in both EA and AA individuals. The 99% credible set contains 2 SNPs and spans an interval of 3,872 bp, a 95% reduction in the number of SNPs and a 91.6% reduction in the length of the credible set interval.

(Figures 2B, 2C, and S4). For example, the narrowed credible region at the *FOXA2* locus, which also overlaps an lncRNA as noted above, falls within an active C3 enhancer cluster and contains binding sites for both NKX2-2 and *FOXA2*, raising the possibility that the causal genetic mechanism at this locus involves regulation of *FOXA2*, the lncRNA at the locus, or both (Figure 2B). The narrowed

regulatory annotation also had genome-wide significant evidence of association in the trans-ethnic analysis (Figure S4). Then, from overlay of Islet Regulome Browser data, we found that 8 of 14 substantially narrowed credible sets for FG and 3 of 9 for FI had either a TFBS or an active islet-specific enhancer within the narrowed credible region

credible region at the *CRY2* locus also overlaps a C3 enhancer cluster in islets that contains an NKX2-2 TFBS (Figure 2C). Furthermore, at three FG loci (*GCK*, *ADCY5* [MIM: 600293], and *GCKR*) and both FI loci (*GCKR* and *PPP1R3B* [MIM: 610541]) whose 99% credible set was narrowed to a single variant, the remaining credible set SNP



**Table 2. Genomic Annotation Characteristics at 22 EA-Associated Type 2 Diabetes Quantitative Traits Loci with Substantially Reduced 99% Credible Sets Based on Trans-ethnic Fine Mapping**

Locus <sup>b</sup>	# SNPs <sup>c</sup>	dbSNP				ENCODE <sup>23</sup>				Islet Regulome Browser <sup>13,a</sup>	
		Syn	Non-Syn	Intronic	eQTL	TF Motif	TFBS	Promoter	Enhancer	DHS	PIACT <sup>d</sup>
<b>Fasting Glucose-Associated Loci</b>											
<i>FOXA2</i>	2	0	0	1	0	2	2	2	2	2	AT
<i>GCK</i>	1	0	0	0	1	1	0	0	1	1	PT
<i>KL</i>	147	1	0	53	24	122	19	18	94	36	PIACT
<i>ADCYS</i>	1	0	0	1	0	0	0	1	1	1	T
<i>GCKR</i>	1	0	0	1	1	1	1	0	1	0	I
<i>PROX1</i>	5	0	0	0	6	5	1	1	4	1	PAT
<i>DPYSL5</i>	50	1	1	37	23	44	7	9	42	24	PIACT
<i>IGF2BP2</i>	38	0	0	30	32	34	8	8	35	15	PIACT
<i>CDKN2B-ANRIL</i>	5	0	0	0	3	5	0	0	4	2	AT
<i>ADRA2</i>	26	0	0	0	1	22	0	1	12	6	IT
<i>TCF7L2</i>	4	0	0	3	0	2	0	1	3	2	AT
<i>FADS1</i>	16	0	0	12	16	15	7	6	16	10	PAT
<i>DGKB-TMEM195</i>	10	0	0	0	2	8	0	3	10	0	A
<i>CRY2</i>	2	0	0	1	2	2	0	1	2	0	PACT
<b>Fasting Insulin-Associated Loci</b>											
<i>ARL15</i>	22	0	0	22	18	18	3	3	17	5	IT
<i>PPP1R3B</i>	1	0	0	1	1	1	0	0	1	0	-
<i>COBLL1-GRB14</i>	3	0	1	0	3	3	1	0	1	0	T
<i>IRS1</i>	13	0	0	0	13	11	1	0	7	2	C
<i>GCKR</i>	1	0	0	1	1	1	1	0	1	0	I
<i>FAM13A</i>	21	0	0	21	18	15	3	8	20	6	PIACT
<i>ANKRD55-MAP3K1</i>	200	0	0	0	63	161	20	17	147	67	IAT
<i>UHRF1BP1</i>	9	0	0	8	9	8	2	0	4	5	PAT
<i>PPARG</i>	11	0	1	10	11	8	2	4	11	5	-

Abbreviations are as follows: Syn, synonymous SNP; non-syn, non-synonymous SNP; eQTL, expression quantitative trait loci; TF motif, transcription factor motif; TFBS, transcription factor binding site; DHS, DNase I-hypersensitive sites.

<sup>a</sup>The information was obtained on December 1, 2014.

<sup>b</sup>For ease of comparison to previous studies, the loci (13 fasting glucose, 8 fasting insulin, and 1 more for both) are named based on the historically identified nearest protein-coding gene or genes to the index SNP in EA.

<sup>c</sup>#SNPs: the number of SNPs in trans-ethnic analysis-based 99% credible set.

<sup>d</sup>PIACT: P, I, A, C, and T represent promoter, inactive enhancer, active enhancer, CTCF insulator, and transcription factor binding site (TFBS), respectively.

overlapped with regulatory annotation in either ENCODE, Roadmap, or the Islet Regulome (Table 2). Based on data derived from the Islet Regulome Browser, all 14 FG and 7 of 9 FI loci had evidence of regulatory function in pancreatic islets within the credible set (Table 2). Nearly all loci with narrowed credible sets contained at least one transcription factor (TF) motif within the 99% credible set (13/14 FG and 9/9 FI) and had at least one variant associated with *cis*-eQTL data (11/14 FG and all 9 FI). In addition, all 14 FG and 9 FI loci contained some regulatory evidence; in contrast, only three of the loci (*DPYSL5*, *COBLL1-GRB14*, and *PPARG*) contained a nonsynonymous variant in their credible sets (Table 2).

### Relevance of European T2D QT Loci for African Americans

To evaluate the relevance in AA individuals of genetic determinants of FG and FI identified from EA studies, we examined SNP and locus association transferability, allele frequency differences, and patterns of association between FG/FI SNPs and glycemia-related traits. We tested SNP transferability (defined as whether the index EA SNP was associated with the same trait in AA, with the same direction of effect, and  $p < 0.05$ ) at 54 EA-associated FG or FI loci. Of 36 EA FG index SNPs, 11 SNPs reached SNP transferability criteria (binomial  $p = 9.87 \times 10^{-8}$  for observing 11/36 meeting SNP transferability criteria) (Table 3). Of

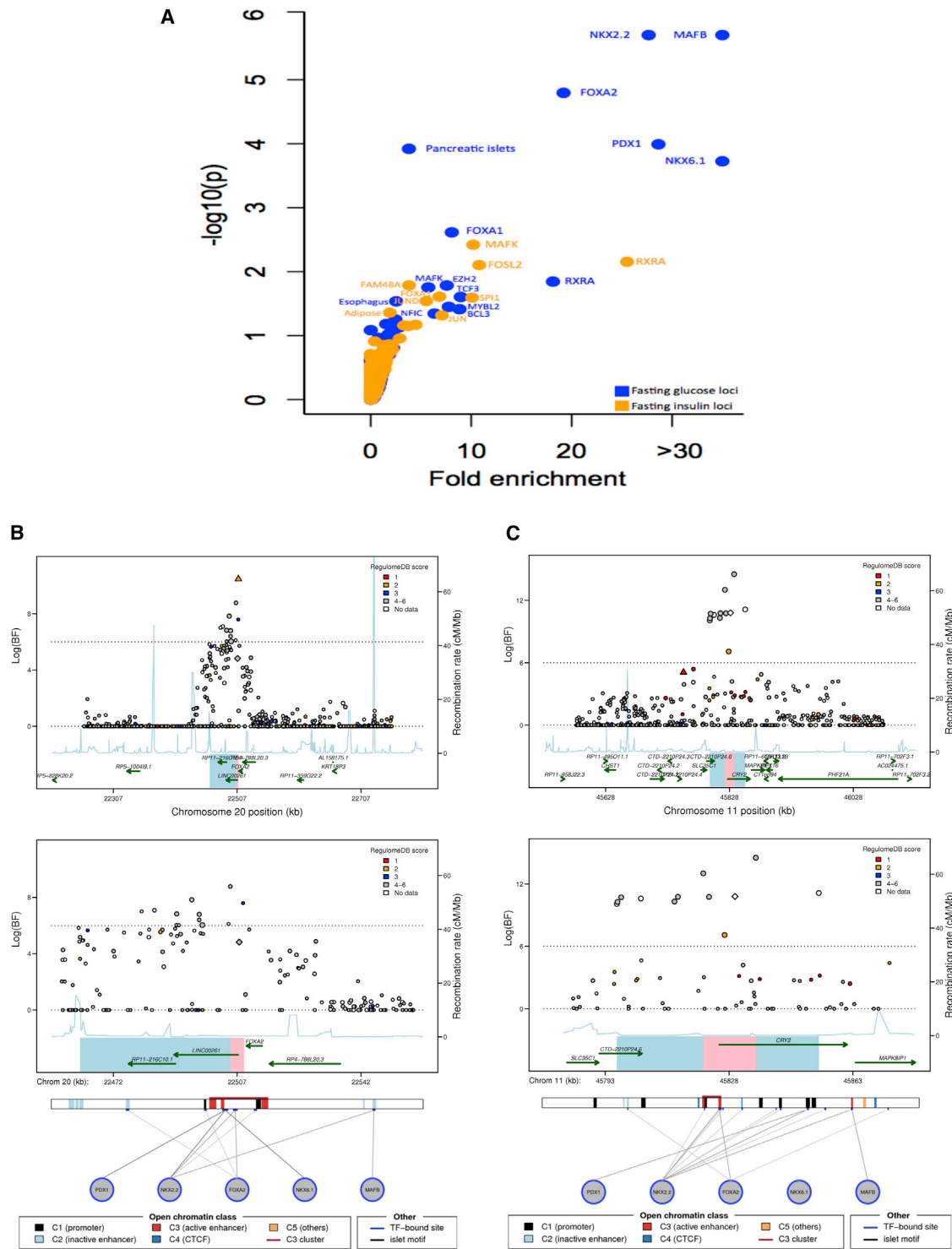


**Figure 2. Trans-ethnic Fine-Mapping of Glycemic Quantitative Trait Loci Highlights Overlap between Trait-Associated SNPs and Predicted Regulatory Function**

(A) Analysis for enrichment of posterior probabilities in SNPs overlapping transcription factor binding sites (TFBSs) and cell-type-specific enhancer and promoter marks at 22 (13 FG, 8 FI, and 1 both FG and FI) substantially narrowed 99% credible sets. x axis shows fold-enrichment above null, the y axis shows  $-\log_{10}(P)$  for enrichment, and FI and FG are indicated by yellow and blue points, respectively. TFBSs and cell types with enhancer or promoter marks with p value for enrichment below 0.01 are labeled.

(B) Regional association plots for fasting glucose after trans-ethnic analysis demonstrating overlap between regulatory annotation and narrowed credible regions at the *FOXA2* locus.

(C) Regional association plots for fasting glucose after trans-ethnic analysis demonstrating overlap between regulatory annotation and narrowed credible regions at the *CRY2* locus.

(legend continued on next page)

18 EA index FI SNPs, 2 met SNP transferability criteria (Table 3). We also found excess concordance in direction of effect of the SNPs comparing EA with AA samples, irrespective of the strength of association: of 36 EA FG index SNPs, 28 SNPs shared the same direction of effect in the AA sample (binomial  $p = 5.97 \times 10^{-4}$ ); of 18 EA FI index SNPs, 14 SNPs shared the same direction of effect in the AA sample (binomial  $p = 0.015$ ) (Figure S5). For both traits, SNPs that met transferability criteria tended to have larger effect sizes than those not meeting the criteria, and the magnitudes of effect in EA were similar to those in AA samples (Figure S5). There was genome-wide excess of directional concordance of SNP effects comparing EA with AA (binomial  $p = 0.021$  for FG and binomial  $p = 0.016$  for FI) when considering SNPs independent of previously reported T2D QT associations and with  $p \leq 0.01$  in EA (Table S8). This evidence supports the hypothesis that trans-ethnic meta-analysis in large samples could reveal additional SNPs associated with glycemic traits.

We also evaluated locus transferability (defined as whether any SNP within  $\pm 250$  kb of the index EA SNP was associated with the same trait in AA at a Bonferroni-corrected  $p < 0.05$ ) at the 54 EA-associated FG or FI loci. Loci were transferable from the EA to AA individuals (adjusting for the effective number of SNPs tested in each region) for 15/38 FG loci and for 10/18 FI loci (Table 4, Figure S2). At six FG loci (*GCK*, *ADCY5*, *GCKR*, *CRY2*, *PPP1R3B*, and *MTNR1B* [MIM: 600804]) and two FI loci (*PDGFC* [MIM: 608452] and *GCKR*), the index SNPs from the EA sample and the most significantly associated SNPs in the AA sample were either in LD ( $r^2 \geq 0.20$ ) in YRI or were the same SNP (Table 4). In contrast, for the remaining loci, the index SNP from the EA sample and the most associated SNP in the AA sample were not in LD ( $r^2 < 0.20$  in AA sample). For these loci with low LD between EA index SNP and the most associated AA SNP, we found a change in effect size  $> 10\%$  for the AA SNP after conditioning on the index SNP in EA at only three FG loci (*SLC30A8* [MIM: 611145], *PPP1R3B*, and *GCK*) (Table S9). These results show ancestrally derived allelic heterogeneity giving more than one variant signal at these FG loci.

#### Allele Frequency Differences and Selection

FG-raising (38 SNPs) and FI-raising (18 SNPs) allele frequencies for EA index SNPs differed widely comparing AA with EA populations (absolute allele frequency differences ranged from 0.007 to 0.825 for FG index SNPs and 0.017 to 0.540 for FI index SNPs) (Table S10, Figure S5). We estimated Wright's fixation index ( $F_{ST}$ )<sup>26</sup> to demonstrate whether selection pressure has resulted in widely different allele frequencies at any SNPs in AA versus EA

populations.  $F_{ST}$  estimates were consistent with moderate to substantial population differentiation for a minority of FG and FI SNPs:  $F_{ST} > 0.15$  at four FG loci (*ADRA2A* [MIM: 104210], *PCSK1* [MIM: 162150], *OR4S1*, and *ARAP1* [MIM: 606646]) and at one FI locus (*UHRF1BP1*) in the AAGILE and MAGIC data. There was also evidence of recent positive selection (absolute value of  $iHS > 2$ ) for one FG locus (*FOXA2*) and three FI loci (*UHRF1BP1*, *HIP1* [MIM: 601767], and *MAP3K19*) in the EA, yet no evidence of recent selection in AA (Table S10).

#### Associations between FG/FI SNPs and Insulin Resistance-Related Metabolic Traits

Many FG/FI-associated loci identified in EA samples were also associated with T2D and other insulin resistance-related traits.<sup>8,9</sup> We investigated these associations in AA individuals at 25 SNPs, including 24 AA SNPs (14 FG, 9 FI, and 1 associated with both FG and FI) at loci that showed transferability, plus the previously undescribed FI SNP (rs6450057) described in the next section. A second FI SNP (also described in the next section), rs213676, was not interrogated for association with metabolic traits due to scant chromosome X data. Table S11 summarizes the association results of these 25 FG/FI SNPs with T2D, body mass index (BMI), BMI-adjusted waist-to-hip ratio (WHR), blood pressure, hypertension (HTN), and lipid levels in AA from several consortia.<sup>32–36,42</sup> 14 of 25 (56%) FG/FI SNPs were associated with T2D or an insulin resistance-related trait ( $p < 0.05$  with an effect in the expected direction [e.g., FG-raising SNP associated with increased risk of T2D]). Six SNPs (24%; 4 [*ADCY5*, *RREB1* (MIM: 602209), *MTNR1B* (MIM: 600804), and *FOXA2*] of 15 FG SNPs and 2 [*COBLL1-GRB14* and *ARL15*] of 11 FI SNPs) were associated with higher odds of T2D in AA samples (n up to 23,818).<sup>31</sup> 40% (6/15) of the FG-raising alleles and 45% (5/11) of the FI-raising alleles were associated with insulin resistance-related traits in AA samples. The FI SNP rs6717858 (*COBLL1-GRB14*) was associated with three traits (T2D, BMI-adjusted WHR, and HDL-C). rs17811863 (*PDGFC*), also an FI SNP, was associated with both systolic and diastolic blood pressure.

#### Previously Undescribed Glycemic Quantitative Trait Loci

The strategy we used for glycemic loci discovery in AAGILE is shown in Figure S1. Results of the discovery analysis are shown in Figure S6. AAGILE GWAS results were combined with MAGIC EA GWAS results<sup>10</sup> in a two-stage meta-analysis approach. In the discovery stage, results from 16 studies (n = 20,209) in the AAGILE AA GWAS fixed effects meta-analysis were combined with results from 29 studies

---

(B and C) The index SNP in European ancestry (MAGIC) is represented by a diamond; the best SNP in African ancestry (AAGILE) is represented by a triangle. SNPs are colored according to the score assigned in RegulomeDB<sup>11</sup> with lower score corresponding to stronger level of evidence supporting regulatory function; data from the Islet Regulome Browser<sup>13</sup> for the genomic interval is shown below regional association plots. The interval spanned by the 99% credible set using EA data only is represented by combining blue and pink regions; interval spanned by the narrowed 99% credible set after trans-ethnic analysis is shown in pink.

---

**Table 3. SNP Transferability in AA Individuals at 13 EA-Associated Type 2 Diabetes Quantitative Trait SNPs**

Locus <sup>b</sup>	Index SNP <sup>c</sup>	Chr	Alleles <sup>d</sup>	EA Association <sup>a</sup>			AA Association <sup>a</sup>			
				EA <sup>e</sup>	Effect <sup>f</sup>	SE	EA <sup>e</sup>	Effect <sup>f</sup>	SE	p
<b>Fasting Glucose-Associated Loci</b>										
<i>MTNR1B</i>	rs10830963	11	G/C	0.30	0.067	0.003	0.08	0.089	0.012	$9.29 \times 10^{-15}$
<i>G6PC2</i>	rs560887	2	C/T	0.70	0.075	0.003	0.93	0.059	0.013	$2.67 \times 10^{-06}$
<i>ADCY5</i>	rs11708067	3	A/G	0.78	0.027	0.003	0.85	0.036	0.008	$6.27 \times 10^{-06}$
<i>GCKR</i>	rs780094	2	C/T	0.62	0.029	0.003	0.82	0.032	0.008	$2.03 \times 10^{-05}$
<i>GCK</i>	rs4607517	7	A/G	0.16	0.062	0.004	0.11	0.041	0.010	$6.84 \times 10^{-05}$
<i>GLIS3</i>	rs7034200	9	A/C	0.49	0.018	0.003	0.63	0.019	0.006	$1.82 \times 10^{-03}$
<i>KL</i>	rs576674	13	G/A	0.15	0.017	0.003	0.60	0.018	0.006	$2.06 \times 10^{-03}$
<i>SLC30A8</i>	rs13266634	8	C/T	0.68	0.027	0.004	0.90	0.024	0.010	$1.82 \times 10^{-02}$
<i>MADD</i>	rs7944584	11	A/T	0.75	0.021	0.003	0.95	0.029	0.014	$3.37 \times 10^{-02}$
<i>DGKB-TMEM195</i>	rs2191349	7	T/G	0.52	0.030	0.003	0.60	0.013	0.006	$3.70 \times 10^{-02}$
<i>GRB10</i>	rs6943153	7	T/C	0.34	0.015	0.002	0.68	0.012	0.006	$4.81 \times 10^{-02}$
<b>Fasting Insulin-Associated Loci<sup>g</sup></b>										
<i>COBLL1-GRB14</i>	rs7607980	2	T/C	0.87	0.027	0.004	0.84	0.042	0.008	$2.85 \times 10^{-07}$
<i>GCKR</i>	rs780094	2	C/T	0.62	0.032	0.004	0.82	0.025	0.008	$1.92 \times 10^{-03}$

SNP transferability is defined as the association  $p < 0.05$  in AA and sharing the same trait-raising allele between EA and AA. 13 EA-identified T2D QT SNPs in 12 loci, including 10 fasting glucose loci, 1 fasting insulin locus, and 1 locus associated with both.

<sup>a</sup>EA Association results refer to the association results using samples of European ancestry in previous publications;<sup>8–10</sup> AA Association results refer to the association results using AAGILE samples of African ancestry assembled in this study.

<sup>b</sup>For ease of comparison to previous studies, the loci are named based on the historically identified nearest protein-coding gene or genes to the index SNP in European ancestry.

<sup>c</sup>Index SNPs are the most significant SNPs previously reported in MAGIC publications. All of these SNPs reach genome-wide significant level ( $p < 5 \times 10^{-8}$ ) in the original study.

<sup>d</sup>EA trait-raising allele/other allele.

<sup>e</sup>Frequency of EA trait-raising allele.

<sup>f</sup>Effect of EA trait-raising allele ([mmol/L] for fasting glucose and [pmol/L] for fasting insulin per trait-raising allele).

<sup>g</sup>The association with BMI-adjusted fasting insulin.

( $n = 57,292$ ) from the MAGIC EA GWAS<sup>10</sup> for trans-ethnic meta-analysis using MANTRA. A total of 62 SNPs met pre-specified multi-tiered criteria for stage 2 follow-up, with 12 SNPs in tier 1, 10 in tier 2, and 40 in tier 3 (Figure S1 and Table S12). Follow-up in the second stage, with up to 10,096 additional AA samples from 14 studies (Table S1), yielded two previously undescribed SNPs in loci associated with FI that exceeded GWAS significance thresholds (Table 5). We found no previously unknown FG loci.

In the fixed effects meta-analysis of AA samples, we identified a previously undescribed SNP (rs213676) on chromosome X near *FAM133A* associated with FI ( $p = 2.4 \times 10^{-8}$ ) (Figure 3A). This FI SNP was not included in the trans-ethnic meta-analysis because MAGIC<sup>10</sup> did not report chromosome X results. Although rs213676 is in a region without known genes, this region might be of regulatory significance because it is known to harbor a TFBS in pancreatic islets<sup>11,13</sup> (Figure 3A).

The other previously undescribed FI SNP, rs6450057 on chromosome 5 (Figure 3B), resides near four putative lncRNA genes and the *PELO* (MIM: 605757) (or *ITGAI* [MIM: 192968]) gene. In trans-ethnic analyses, this locus achieved genome-wide significance ( $\log(\text{BF}) = 7.1$ ) and

trans-ethnic fine-mapping reduced the credible set at this locus from 229 SNPs to just 3 SNPs. Interestingly, the rs6450057 T allele is associated with higher FI ( $p = 3.1 \times 10^{-6}$ ) in AA samples but with lower FI ( $p = 9.2 \times 10^{-5}$ ) in EA samples in ancestry-specific fixed-effect meta-analyses (Table 5). The discordant direction of effect at this locus was observed across nearly all SNPs at the locus, regardless of LD with rs6450057 (Figure 3C). However, the direction of effects did not show a clear pattern in the association analysis after conditioning on rs6450057, implying that the signal at this locus was driven by rs6450057 (Figure S7). As with many of the glycemic QT loci described above, the 99% credible set at this locus did not include coding variants but did overlap an active C3 enhancer in pancreatic islets<sup>11,13</sup> (Figure 3D).

## Discussion

We assembled a large sample of AA individuals, combined resulting data with published data from EA individuals, and used trans-ethnic fine mapping to narrow the genomic interval containing putative causal SNPs for 22 of 54



previously identified FI and FG loci. We demonstrated that many of the genetic variants associated with FG and FI are predicted to have regulatory function, with few having predicted protein-coding function. The results show that although a substantial portion of the genetic architecture underlying these T2D-associated traits is shared across EA and AA populations, allelic heterogeneity suggests that there are also genetic variants unique to AA populations. Finally, we identified two previously undescribed FI loci, bringing to 56 the number of FG- and FI-associated loci in humans.

Fine mapping combined with regulatory annotation provides a plausible functional explanation for the many T2D-associated GWAS loci that reside in non-protein-coding regions of the genome.<sup>43–45</sup> Previous GWAS findings from MAGIC show complete overlap of loci associated with HOMA-B (a measure of beta cell function<sup>46</sup>) and FG,<sup>9</sup> so it would be expected that fine-mapping of FG loci might identify regulatory function in islets. On the other hand, FI is typically considered a marker of insulin resistance.<sup>47</sup> However, insulin resistance does not account for all of the variability in FI,<sup>48,49</sup> and fasting hyperinsulinemia itself, due to hypersecretion of insulin by beta cells, might be causal in the pathogenesis of T2D.<sup>50–52</sup> Our finding that some FI loci had predicted regulatory function in islets is supportive of this evidence. At many loci, for instance at *FOXA2* and *PPP1R3B*, the narrowed credible sets from trans-ethnic analysis coupled with genomic annotation focused attention on lncRNA transcripts rather than the nearest protein-coding gene, by convention generally assumed to be the putative causal transcript. At the *FOXA2* locus, the trans-ethnic credible set combined with genomic annotation highlights regulatory functionality in glycemia-related tissues—enhancer marks and TFBS in pancreas and liver—as well as an lncRNA that might affect *FOXA2* expression, raising two possible causal regulatory mechanisms for altered FG.<sup>12,13,41</sup> Awareness of the regulatory nature of some genetic determinants of FG and FI provides insight into novel approaches for the regulation of glucose homeostasis. In particular, regulatory targets might be amenable to post-genomic manipulation (e.g., by genome editing, use of antisense oligonucleotides, or enzyme hijacking) as suggested in other areas.<sup>53,54</sup> For instance, by knowing that polymorphisms in aldehyde dehydrogenase 2 (*ALDH2*) enzyme are associated with poor alcohol metabolism in some Asian populations, the enzyme hijacking technique has been used to upregulate a related, but naturally unimportant, enzyme (*ALDH3A1*), thereby improving alcohol metabolism and reducing cancer risk in mice.<sup>53</sup> Such techniques could in the future be extended to T2D prevention and control if accessible regulatory pathways are elucidated.

At the *GCKR* locus, trans-ethnic fine mapping provided added information to the prior knowledge of this locus identified from studies in EA populations. The 99% credible set constructed using trans-ethnic analysis results at *GCKR* contained only one non-coding SNP, rs780094

(GenBank: NC\_000002.12; g.27518370T>C), the most strongly FG-associated SNP in both EA and AA. However, prior fine-mapping<sup>39</sup> in EA and functional studies<sup>40</sup> have implicated rs1260326, a nonsynonymous variant (GenBank: NC\_000002.12; g.27508073T>C [p.Leu446Pro]), as a likely causal SNP at this locus. This missense variant was excluded from the narrowed credible set. This could imply that the lead non-coding SNP rs780094, which has strong evidence as residing in a TFBS, is also a causal variant at the locus (Table S5). On the basis of statistical evidence, we were unable to distinguish the association of these two SNPs in EA samples due to high LD ( $r^2 = 0.93$ ). However, in AA the evidence of association with FG was several orders of magnitude stronger for the non-coding SNP, rs780094 ( $p = 2.2 \times 10^{-5}$ ), than the coding SNP, rs1260326 ( $p = 0.03$ ) and their LD is weaker ( $r^2 = 0.47$ ). Both SNPs may play a role at the *GCKR* locus; a causal variant tagged by rs780094 might be common to both ancestries, resulting in the narrowed trans-ethnic credible set observed here, while the nonsynonymous variant rs1260326 might have greater functional impact in EA than in AA individuals. Alternatively, the actual causal SNP could be in LD with both of these SNPs, and more dense imputation or deep sequencing might reveal additional SNPs carried on haplotypes with these SNPs. Since crystal structural analysis of the *GCKR* protein has not identified the 446 residue as critical for binding of regulating molecules (fructose 1-phosphate and fructose 6-phosphate), genetic heterogeneity involving both coding and regulatory functional variation at the locus remains a plausible hypothesis.<sup>55</sup>

Analyses of the relevance of glycemic QT loci in AA suggest that genetic determinants of human glucose regulation are more similar than different across human populations. We observed an excess of consistency in direction of effect of FG and FI SNPs comparing AA with EA, regardless of statistical significance of SNPs in AA, and a substantial portion (50% for FG and 56% for FI) of EA index SNP or loci were transferable to AA individuals. As in previous studies in EA individuals,<sup>8,9</sup> most of the transferable T2D EA loci were also associated with T2D or insulin resistance-related traits in AA individuals, demonstrating common genetic pathways underlying glycemic QTs and other metabolic traits. We also found that several FG-raising and FI-raising alleles were at least nominally associated with lower odds of T2D or “better” metabolic trait profiles in the AA samples. Many of the loci previously observed to have this discordant pattern of associations across traits in EA, including *GCKR*,<sup>9,39,40,56,57</sup> *MADD* (MIM: 603584),<sup>9</sup> *PDGFC*,<sup>10</sup> and *FOXA2*,<sup>10</sup> had a similar pattern in our AA sample, demonstrating that the complexity of the genetic architecture of these traits is shared across populations.

By combining AA with EA information, including chromosome X variants in AA, we identified two previously undescribed FI SNPs near *FAM133A* and *PELO*, increasing the total number of human FG/FI-associated loci from 54 to

**Table 4. Locus Transferability in African Individuals for 24 EA-Identified Type 2 Diabetes Quantitative Traits Associations**

Locus <sup>b</sup>	SNP Information				Best SNP Association							LD <sup>a</sup> in YRI and CEU			
	Index SNP in EA <sup>c</sup>	Best SNP in AA <sup>d</sup>	Best SNP Alleles <sup>e</sup>	EAF <sup>f</sup>	Effect <sub>uc</sub> <sup>g</sup>	SE	p	adj-p <sup>h</sup>	Effect <sub>c</sub> <sup>i</sup>	% Change in Effect <sup>j</sup>	R <sup>2</sup> <sub>YRI</sub>	D' <sub>YRI</sub>	R <sup>2</sup> <sub>CEU</sub>	D' <sub>CEU</sub>	
<b>Fasting Glucose-Associated Loci</b>															
<i>MTNR1B</i>	rs10830963	rs10830963	G/C	0.079	0.089	0.012	$9.3 \times 10^{-15}$	$3.5 \times 10^{-3}$	NA	NA	1.00	1.00	1.00	1.00	
<i>GCK</i>	rs4607517	rs1799884	T/C	0.174	0.047	0.007	$2.0 \times 10^{-10}$	$8.6 \times 10^{-3}$	0.038	19.3	0.47	1.00	1.00	1.00	
<i>G6PC2</i>	rs560887	rs830193	C/T	0.816	0.037	0.008	$1.2 \times 10^{-6}$	$2.9 \times 10^{-3}$	0.035	5.2	0.00	0.08	0.07	0.58	
<i>FOXA2</i>	rs6048205	rs1203907	T/C	0.505	0.027	0.006	$3.7 \times 10^{-6}$	$3.3 \times 10^{-3}$	0.025	7.7	0.18	0.92	0.66	1.00	
<i>RREB1</i>	rs17762454	rs557074	G/T	0.455	0.027	0.006	$4.2 \times 10^{-6}$	$4.1 \times 10^{-3}$	0.025	4.4	0.01	0.48	0.02	0.51	
<i>SLC30A8</i>	rs13266634	rs10505311	G/T	0.837	0.036	0.008	$5.6 \times 10^{-6}$	$3.7 \times 10^{-3}$	0.025	30.8	0.19	1.00	NA	NA	
<i>ADCY5</i>	rs11708067	rs11708067	A/G	0.846	0.036	0.008	$6.3 \times 10^{-6}$	$4.5 \times 10^{-3}$	NA	NA	1.00	1.00	1.00	1.00	
<i>GCKR</i>	rs780094	rs780094	C/T	0.819	0.032	0.008	$2.0 \times 10^{-5}$	$1.4 \times 10^{-2}$	NA	NA	1.00	1.00	1.00	1.00	
<i>CRY2</i>	rs11605924	rs11038651	T/C	0.828	0.033	0.008	$3.8 \times 10^{-5}$	$5.3 \times 10^{-3}$	0.030	9.4	0.55	0.85	0.12	0.44	
<i>MADD</i>	rs7944584	rs1052373	T/C	0.481	0.022	0.006	$1.4 \times 10^{-4}$	$1.1 \times 10^{-2}$	0.022	0.0	NA	NA	0.15	1.00	
<i>PPP1R3B</i>	rs4841132	rs7004769	A/G	0.228	0.024	0.007	$2.7 \times 10^{-4}$	$2.2 \times 10^{-3}$	0.018	26.1	0.44	1.00	0.38	1.00	
<i>PROX1</i>	rs340874	rs2282387	C/G	0.519	0.021	0.006	$4.6 \times 10^{-4}$	$3.4 \times 10^{-3}$	0.021	-1.2	0.01	0.27	0.00	0.09	
<i>IKBKAP</i>	rs16913693	rs7038936	C/T	0.669	0.021	0.006	$5.3 \times 10^{-4}$	$3.9 \times 10^{-3}$	NA <sup>k</sup>	NA	0.04	0.29	0.01	0.39	
<i>ADRA2A</i>	rs10885122	rs12569523	A/T	0.368	0.021	0.006	$5.4 \times 10^{-4}$	$3.6 \times 10^{-3}$	0.020	1.9	0.01	0.11	0.00	0.25	
<i>PCSK1</i>	rs13179048	rs7722200	T/C	0.773	0.023	0.007	$8.2 \times 10^{-4}$	$7.0 \times 10^{-3}$	0.023	-0.9	0.04	1.00	0.66	0.83	
<b>Fasting Insulin-Associated Loci</b>															
<i>COBLL1-GRB14</i>	rs7607980	rs6717858	T/C	0.281	0.036	0.007	$8.6 \times 10^{-8}$	$5.3 \times 10^{-3}$	0.034	6.4	0.06	1.00	0.22	1.00	
<i>ARL15</i>	rs4865796	rs6876198	C/T	0.295	0.031	0.007	$2.0 \times 10^{-6}$	$3.8 \times 10^{-3}$	0.030	4.0	0.11	0.89	0.09	0.87	
<i>PPP1R3B</i>	rs4841132	rs9949	G/A	0.231	0.029	0.007	$6.9 \times 10^{-5}$	$2.2 \times 10^{-3}$	0.027	6.7	0.11	0.51	0.01	0.23	
<i>IRS1</i>	rs2943634	rs4413154	G/A	0.041	0.062	0.016	$1.2 \times 10^{-4}$	$4.9 \times 10^{-3}$	0.062	1.3	0.01	1.00	0.08	1.00	
<i>ANKRD55-MAP3K1</i>	rs459193	rs7700714	A/G	0.436	0.023	0.006	$1.8 \times 10^{-4}$	$2.3 \times 10^{-3}$	0.024	-3.6	0.00	0.03	0.04	0.29	
<i>FAM13A</i>	rs3822072	rs17799176	C/G	0.934	0.043	0.012	$4.3 \times 10^{-4}$	$5.8 \times 10^{-3}$	0.043	0.2	0.00	0.22	0.02	0.43	
<i>HIP1</i>	rs1167800	rs11465341	C/T	0.035	0.060	0.017	$4.5 \times 10^{-4}$	$8.1 \times 10^{-3}$	0.060	0.0	0.00	1.00	NA	NA	
<i>MAP3K19</i>	rs1530559	rs13405563	T/C	0.924	0.043	0.013	$5.5 \times 10^{-4}$	$8.8 \times 10^{-3}$	0.045	-3.6	0.00	0.79	0.04	1.00	
<i>PDGFC</i>	rs4691380	rs17811863	G/A	0.333	0.022	0.006	$6.2 \times 10^{-4}$	$4.7 \times 10^{-3}$	0.020	8.9	0.21	0.49	0.77	0.93	
<i>GCKR</i>	rs780094	rs780094	C/T	0.817	0.025	0.008	$1.9 \times 10^{-3}$	$1.4 \times 10^{-2}$	NA	NA	1.00	1.00	1.00	1.00	

(legend on next page)

<sup>a</sup>LD information between the EA index SNP and the best SNP in AA.

<sup>b</sup>24 EA-identified T2D QT (14 glucose, 9 fasting insulin, and 1 associated with both) loci with locus-wide significant,  $p < 0.05$ /effective number of independent SNPs within each locus, associations. For ease of comparison to previous studies, the loci are named based on the historically identified nearest protein-coding gene or genes to the index SNP in European ancestry.

<sup>c</sup>Index SNPs are the most significant SNPs previously reported in MAGIC publications. All of these SNPs reach genome-wide significant level ( $p < 5 \times 10^{-8}$ ) in the original study.

<sup>d</sup>The best SNP in AA is the most significant SNP within  $\pm 250$  kb region of the EA index SNP.

<sup>e</sup>AA trait-raising allele/other allele.

<sup>f</sup>Frequency of AA trait-raising allele (effect allele) for the best SNP.

<sup>g</sup>Effect of AA trait-raising allele (mmol/L) for fasting glucose and [pmol/L] for fasting insulin per trait-raising allele). This is unconditional association of best SNP in AA samples.

<sup>h</sup>Indicates the  $p$  value is adjusted for locus-wise multiple comparison and calculated as  $\min(I, P)$  \*the number of effective SNPs). The information for the number of effective SNPs is available in Table S8.

<sup>i</sup>Effect<sub>loc</sub> is the association of the best SNP unconditional on the EA index SNP in AA samples and Effect<sub>loc</sub> is the association of AA best SNP conditional on EA index SNP in AA samples.

<sup>j</sup>Percent change in association effect for the best SNP in the AA samples. It is calculated as the (unconditional association effect – conditional association effect)/(unconditional association effect). More detailed information for conditional and unconditional association results are available in Table S8.

<sup>k</sup>The association results for EA index SNP is not available in AA.

56. The lead SNP at the *PELO* locus, rs6450057, had discordant effects in the AA and EA samples: the FI-raising allele in AA lowered FI in EA. Discordant effects of common variants on complex human traits have been observed in other traits such as breast cancer<sup>58</sup> and serum protein levels<sup>59</sup> but not in T2D QT. This may be due to the lack of trans-ethnic study of T2D QT, the use of fixed-effects approaches that do not adequately account for heterogeneity in LD or allelic frequencies across populations, gene-environment interactions with differential exposures across ancestral populations, or gene-gene interactions with substantially different allele frequencies for the interacting variants across ancestries. Alternatively, EA and AA groups may have different causal variants that are in moderate LD with the lead SNP, thus boosting the association signal in trans-ethnic meta-analyses that take account of the heterogeneity in allelic effects between ancestry groups. Haplotype analysis in both EA and AA samples did not clearly elucidate differential SNP contributions to FI levels at the *PELO* locus. Although our analyses are unable to distinguish between possible mechanisms driving the discordant effects of rs6450057 in EA and AA populations, evaluation of the locus, with high-density imputation and/or whole-genome sequencing data from individuals of EA and AA as well as laboratory-based examination of the clustered enhancer in pancreatic islets at this locus, could help explain the observed divergent associations.

A major strength of this investigation was the large sample size of AA, a hitherto under-studied ancestral group with a heavy burden of hyperglycemia, insulin resistance, and T2D. The large sample of AA individuals allowed genome-wide trans-ethnic discovery, fine-mapping, and (combined with new annotation resources) detailed prediction of regulatory function. Yet, despite the large sample size, our study still had modest power to detect loci with small effects. With sample size of 30,305 (discovery + follow up) in AA, we had only 15% power to detect an EA-identified median FG effect size of 0.0196 mmol/L with SD of 0.5 mmol/L, for variants with MAF of 0.3. In addition, the reduced size of LD blocks in AA populations decreased the probability that a tagging SNP resided on the same haplotype as a causal variant, further limiting power for discovery. Also, reduced LD haplotype and corresponding greater genetic diversity made imputation for AA samples more challenging. The HapMap2 panel, used as the imputation panel for majority of contributing studies in this analysis, did not provide complete coverage of common and low-frequency genetic variation in AA samples; the latest reference panels from 1000 Genomes Phase 3 should provide better coverage although whole-genome sequencing and laboratory analysis of genetic function are going to be necessary to unequivocally determine causal variants that may have similar or different effects across ancestral groups. As for other trans-ethnic efforts,<sup>16,60</sup> we have reported the improvement in fine-mapping resolution in terms of the reduction in the number of SNPs or the length of the genomic interval to which they

**Table 5. Two Previously Undescribed Loci Associated with Fasting Insulin in African Ancestry Individuals**

SNP <sup>a</sup>	Chr	Position (build 36)	Nearest Gene	Alleles <sup>b</sup>	African Ancestry Association <sup>c</sup>			European Ancestry Association			Trans-ethnic Association		
					N <sub>AA</sub> <sup>d</sup>	EAF <sup>e</sup>	P	N <sub>EA</sub> <sup>d</sup>	EAF <sup>e</sup>	P	N <sub>Total</sub> <sup>d</sup>	log(BF)	
rs213676	X	93358147	FAM133A	C/G	14,043	0.98	0.147	2.37 × 10 <sup>-8</sup>	0 <sup>8</sup>	NA	NA	14,043	6.26
rs6450057	5	51683121	PELO	T/C	20,853	0.4	0.027	3.11 × 10 <sup>-6</sup>	52,372	0.37	-0.011	73,225	7.1

<sup>a</sup>Two SNPs in previously undescribed loci are associated with fasting insulin at genome-wide significance, i.e.,  $p < 5 \times 10^{-8}$  in AA individuals or with  $\log\text{BF} > 6$  in trans-ethnic meta-analysis.

<sup>b</sup>Trait-raising allele/other allele in the sample of African ancestry.

<sup>c</sup>Association results from the samples of African ancestry based on the joint analysis of samples from stage 1 and stage 2.

<sup>d</sup>N<sub>AA</sub>: the sample size of African ancestry; N<sub>EA</sub>: the sample size of European ancestry; N<sub>Total</sub>: total sample size of EA and AA.

<sup>e</sup>Frequency of effect allele (i.e., AA trait-raising allele).

<sup>f</sup>Effect of AA trait-raising allele (Jpmol/L) per trait-raising allele).

<sup>g</sup>Association analysis result is unavailable in MAGIC EA samples because the original MAGIC<sup>10</sup> effort analyzed only autosomal variants.

map. The improvement from trans-ethnic analysis varied from one locus to another as shown in Table S2. We used 20% reduction in credible set size to provide an overall assessment of fine-mapping resolution (albeit crude). However, fine-mapping resolutions depends on many factors, such as the size of LD blocks and the availability of high-quality read-depth for the reference datasets used in the imputation, and will therefore vary from one locus to another. Furthermore, the improvement in resolution offered by trans-ethnic meta-analysis relies on the extent of LD differences with the causal variant between ancestry groups and the increase in sample size. However, importantly, credible set sizes can increase after trans-ethnic meta-analysis, which most often occurs due to different underlying causal variants across ancestry groups. In this scenario, the credible set captures multiple association signals driven by each causal variant, which will therefore be larger than that observed for ethnic-specific analyses.

In conclusion, by using AA and EA trans-ethnic analysis, we narrowed the genomic interval containing likely causal variants for a large number of biologically plausible FG and FI loci and demonstrated that many FG and FI loci probably have regulatory, rather than protein-coding, function. The observed effects of genetic variants on glycemic traits might result from multiple regulatory functions residing in the same genomic region; for example, concurrent presence of an enhancer and lncRNA at the FOXA2 locus, an attribute that could lead to synergy in function. We also showed that there are probably both shared and unique genetic determinants of T2D QTs across European and African ancestral populations. We identified two previously undescribed FI loci, bringing the total number of identified FG and FI loci in humans to 56. Our finding of the predicted regulatory significance of many FG and FI loci is particularly noteworthy, given the prior uncertainty about the functional relevance of most GWAS findings for T2D and related QTs. Our study provides a framework for further follow-up of GWAS signals seen in EA and other ancestral populations. This approach using trans-ethnic meta-analysis for discovery and transferability combined with trans-ethnic fine-mapping and state-of-the-art annotation will lead the way to an understanding of the functional, and ultimately therapeutic, implications of genetic variation underlying glucose homeostasis, T2D risk, and other complex disorders.

### Supplemental Data

Supplemental Data include consortium membership, sources of data, author contributions, acknowledgments, 7 figures, and 12 tables and can be found with this article online at <http://dx.doi.org/10.1016/j.ajhg.2016.05.006>.

### Conflicts of Interest

B.M.P. serves on the DSMB of a clinical trial for the device manufacturer Zoll LifeCor and on the Steering Committee for the Yale



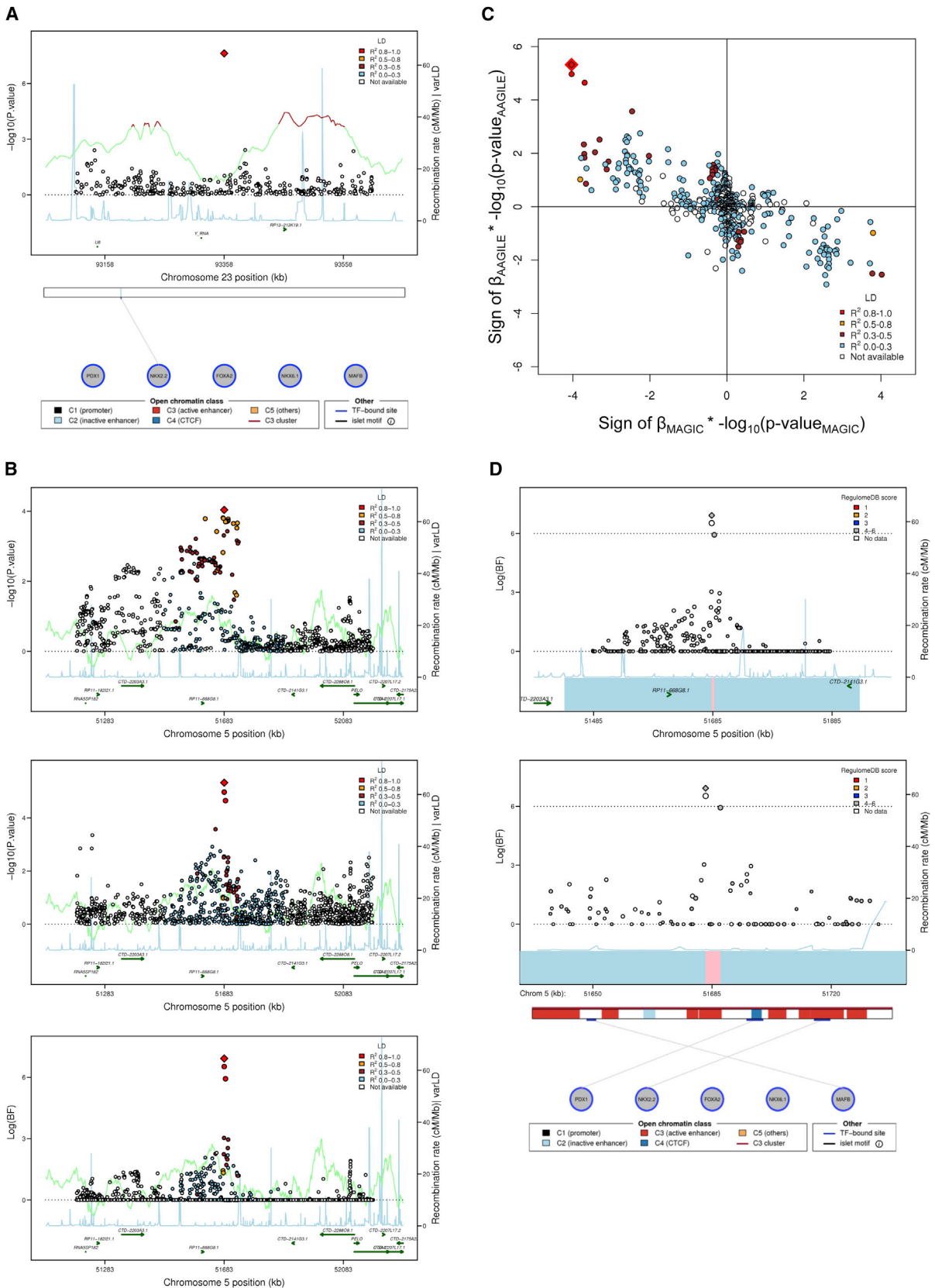


**Figure 3. Regional Association Plots and Functional Annotation for Two Previously Undescribed Loci**

(A) Regional association plot of a previously undescribed chromosome X locus associated with fasting insulin in AA individuals. The nearest gene is *FAM133A*. Top panel shows association signal on the y axis ( $-\log(P)$ ) and genomic position on chromosome X on the x axis. The red diamond data point represents the lead SNP (rs213676) within the region. The blue line represents the recombination

(legend continued on next page)

Open Data Access Project funded by Johnson & Johnson. D.V. is a consultant for Consumable Science, Inc. J.R.K. holds stock in Pfizer, Inc., and Gilead Sciences, Inc.

Received: February 8, 2016

Accepted: May 2, 2016

Published: June 16, 2016

## Web Resources

AAGILE consortium, <http://aagileandmedia.partners.org/>  
HaploReg, <http://www.broadinstitute.org/mammals/haploreg/haploreg.php>  
Human Islet Regulome Browser, <http://isletregulome.org/>  
OMIM, <http://www.omim.org/>  
RefSeq, <http://www.ncbi.nlm.nih.gov/RefSeq>

## References

1. Danaei, G., Finucane, M.M., Lu, Y., Singh, G.M., Cowan, M.J., Paciorek, C.J., Lin, J.K., Farzadfar, F., Khang, Y.H., Stevens, G.A., et al.; Global Burden of Metabolic Risk Factors of Chronic Diseases Collaborating Group (Blood Glucose) (2011). National, regional, and global trends in fasting plasma glucose and diabetes prevalence since 1980: systematic analysis of health examination surveys and epidemiological studies with 370 country-years and 2.7 million participants. *Lancet* 378, 31–40.
2. Spanakis, E.K., and Golden, S.H. (2013). Race/ethnic difference in diabetes and diabetic complications. *Curr. Diab. Rep.* 13, 814–823.
3. Cheng, C.Y., Reich, D., Haiman, C.A., Tandon, A., Patterson, N., Selvin, E., Akyzbekova, E.L., Brancati, F.L., Coresh, J., Boerwinkle, E., et al. (2012). African ancestry and its correlation to type 2 diabetes in African Americans: a genetic admixture analysis in three U.S. population cohorts. *PLoS ONE* 7, e32840.
4. Rosenberg, N.A., Huang, L., Jewett, E.M., Szpiech, Z.A., Jan-kovic, I., and Boehnke, M. (2010). Genome-wide associa-
- tion studies in diverse populations. *Nat. Rev. Genet.* 11, 356–366.
5. Fesinmeyer, M.D., Meigs, J.B., North, K.E., Schumacher, F.R., Bůžková, P., Franceschini, N., Haessler, J., Goodloe, R., Spencer, K.L., Voruganti, V.S., et al. (2013). Genetic variants associated with fasting glucose and insulin concentrations in an ethnically diverse population: results from the Population Architecture using Genomics and Epidemiology (PAGE) study. *BMC Med. Genet.* 14, 98.
6. Rasmussen-Torvik, L.J., Guo, X., Bowden, D.W., Bertoni, A.G., Sale, M.M., Yao, J., Bluemke, D.A., Goodarzi, M.O., Chen, Y.I., Vaidya, D., et al. (2012). Fasting glucose GWAS candidate region analysis across ethnic groups in the Multi-ethnic Study of Atherosclerosis (MESA). *Genet. Epidemiol.* 36, 384–391.
7. Liu, C.T., Ng, M.C., Rybin, D., Adeyemo, A., Bielinski, S.J., Boerwinkle, E., Borecki, I., Cade, B., Chen, Y.D., Djousse, L., et al. (2012). Transferability and fine-mapping of glucose and insulin quantitative trait loci across populations: CARE, the Candidate Gene Association Resource. *Diabetologia* 55, 2970–2984.
8. Scott, R.A., Lagou, V., Welch, R.P., Wheeler, E., Montasser, M.E., Luan, J., Mägi, R., Strawbridge, R.J., Rehnberg, E., Gustafsson, S., et al.; DIAbetes Genetics Replication and Meta-analysis (DIAGRAM) Consortium (2012). Large-scale association analyses identify new loci influencing glycemic traits and provide insight into the underlying biological pathways. *Nat. Genet.* 44, 991–1005.
9. Dupuis, J., Langenberg, C., Prokopenko, I., Saxena, R., Soranzo, N., Jackson, A.U., Wheeler, E., Glazer, N.L., Bouatia-Naji, N., Gloyn, A.L., et al.; DIAGRAM Consortium; GIANT Consortium; Global BPgen Consortium; Anders Hamsten on behalf of Procardis Consortium; MAGIC investigators (2010). New genetic loci implicated in fasting glucose homeostasis and their impact on type 2 diabetes risk. *Nat. Genet.* 42, 105–116.
10. Manning, A.K., Hivert, M.F., Scott, R.A., Grimsby, J.L., Bouatia-Naji, N., Chen, H., Rybin, D., Liu, C.T., Bielak, L.F., Prokopenko, I., et al.; DIAbetes Genetics Replication And Meta-analysis (DIAGRAM) Consortium; Multiple Tissue

rate. The color of each data point indicates its LD value ( $r^2$ ) with the lead SNP at the locus based on HapMap2 YRI: white,  $r^2$  not available; blue,  $r^2 = 0.0-0.2$ ; brown,  $r^2 = 0.2-0.5$ ; orange,  $r^2 = 0.5-0.8$ ; red,  $r^2 = 0.8-1.0$ . The bottom part of the figure shows Islet Regulome Browser data<sup>13</sup> for the genomic interval shown in the regional association plot.

(B) Regional association plot of a previously undescribed chromosome 5 locus associated with fasting insulin in trans-ethnic meta-analysis. The nearest gene is *PELO* (also called *ITGAI*). The red diamond data point represents the lead SNP (rs6450057) within the region. The blue line represents the recombination rate. The color of each data point indicates its LD value ( $r^2$ ) with the lead SNP at the locus based on HapMap2: white,  $r^2$  not available; blue,  $r^2 = 0.0-0.2$ ; brown,  $r^2 = 0.2-0.5$ ; orange,  $r^2 = 0.5-0.8$ ; red,  $r^2 = 0.8-1.0$ . The top two panels show association with  $-\log(P)$  on the y axis and genomic position on chromosome 5 on the x axis. The top panel shows association in European ancestry (EA) individuals in MAGIC with plotted points colored according to LD with the lead SNP in HapMap CEU individuals; the middle panel shows association in African ancestry (AA) samples with plotted points colored according to LD with lead SNP in HapMap YRI individuals. The bottom panel shows the trans-ethnic association, with  $\log(BF)$  on the y axis and genomic position on the x axis, and plotted points colored according to LD with lead SNP in HapMap YRI individuals.

(C) Comparison of the direction of effect on fasting insulin levels of SNPs at the previously undescribed chromosome 5 locus (*PELO*) comparing EA with AA samples. The product of the sign of the beta-coefficient for FI level and  $-\log(P)$  for each SNP at the locus in EA samples (MAGIC) and in AA samples (AAGILE) is plotted on the x and y axes, respectively. The red diamond data point represents the lead SNP (rs6450057) within the region. The color of each data point indicates its LD value ( $r^2$ ) with the lead SNP at the locus based on HapMap2 YRI: white,  $r^2$  not available; blue,  $r^2 = 0.0-0.2$ ; brown,  $r^2 = 0.2-0.5$ ; orange,  $r^2 = 0.5-0.8$ ; red,  $r^2 = 0.8-1.0$ . SNPs exhibit opposite effects on fasting insulin level with similar association p values across the LD spectrum at the locus.

(D) Regional association plot of a previously undescribed chromosome 5 locus, with plotted points colored according to RegulomeDB score. The diamond data point represents the lead SNP (rs6450057) within the region; the 99% credible set derived from EA data only is represented by combining the blue and pink boxes; the 99% credible set derived from trans-ethnic analysis is represented by the pink box. Top panel shows a 500 kb genomic span, the lower panel shows a 100 kb genomic span. Data from the Islet RegulomeDB, aligned in the bottom part of the panel, shows binding sites for five transcription factors and regulatory genomic marks in pancreatic islets.

- Human Expression Resource (MUTHER) Consortium (2012). A genome-wide approach accounting for body mass index identifies genetic variants influencing fasting glycemic traits and insulin resistance. *Nat. Genet.* *44*, 659–669.
11. Boyle, A.P., Hong, E.L., Hariharan, M., Cheng, Y., Schaub, M.A., Kasowski, M., Karczewski, K.J., Park, J., Hitz, B.C., Weng, S., et al. (2012). Annotation of functional variation in personal genomes using RegulomeDB. *Genome Res.* *22*, 1790–1797.
  12. Ward, L.D., and Kellis, M. (2012). HaploReg: a resource for exploring chromatin states, conservation, and regulatory motif alterations within sets of genetically linked variants. *Nucleic Acids Res.* *40*, D930–D934.
  13. Pasquali, L., Gaulton, K.J., Rodríguez-Seguí, S.A., Mularoni, L., Miguel-Escalada, I., Akerman, I., Tena, J.J., Morán, I., Gómez-Marín, C., van de Bunt, M., et al. (2014). Pancreatic islet enhancer clusters enriched in type 2 diabetes risk-associated variants. *Nat. Genet.* *46*, 136–143.
  14. Lizio, M., Harshbarger, J., Shimoji, H., Severin, J., Kasukawa, T., Sahin, S., Abugessaisa, I., Fukuda, S., Hori, F., Ishikawa-Kato, S., et al.; FANTOM consortium (2015). Gateways to the FANTOM5 promoter level mammalian expression atlas. *Genome Biol.* *16*, 22.
  15. Morris, A.P. (2011). Transethnic meta-analysis of genomewide association studies. *Genet. Epidemiol.* *35*, 809–822.
  16. Mahajan, A., Go, M.J., Zhang, W., Below, J.E., Gaulton, K.J., Ferreira, T., Horikoshi, M., Johnson, A.D., Ng, M.C., Prokopenko, I., et al.; DIABetes Genetics Replication And Meta-analysis (DIAGRAM) Consortium; Asian Genetic Epidemiology Network Type 2 Diabetes (AGEN-T2D) Consortium; South Asian Type 2 Diabetes (SAT2D) Consortium; Mexican American Type 2 Diabetes (MAT2D) Consortium; Type 2 Diabetes Genetic Exploration by Nex-generation sequencing in multi-Ethnic Samples (T2D-GENES) Consortium (2014). Genome-wide trans-ancestry meta-analysis provides insight into the genetic architecture of type 2 diabetes susceptibility. *Nat. Genet.* *46*, 234–244.
  17. Devlin, B., and Roeder, K. (1999). Genomic control for association studies. *Biometrics* *55*, 997–1004.
  18. Howie, B., Fuchsberger, C., Stephens, M., Marchini, J., and Abecasis, G.R. (2012). Fast and accurate genotype imputation in genome-wide association studies through pre-phasing. *Nat. Genet.* *44*, 955–959.
  19. Willer, C.J., Li, Y., and Abecasis, G.R. (2010). METAL: fast and efficient meta-analysis of genomewide association scans. *Bioinformatics* *26*, 2190–2191.
  20. Hong, J., Lunetta, K.L., Cupples, L.A., Dupuis, J., and Liu, C.T. (2016). Evaluation of a two-stage approach in trans-ethnic meta-analysis in genome-wide association studies. *Genet. Epidemiol.* *40*, 284–292.
  21. Maller, J.B., McVean, G., Byrnes, J., Vukcevic, D., Palin, K., Su, Z., Howson, J.M., Auton, A., Myers, S., Morris, A., et al.; Wellcome Trust Case Control Consortium (2012). Bayesian refinement of association signals for 14 loci in 3 common diseases. *Nat. Genet.* *44*, 1294–1301.
  22. Kundaje, A., Meuleman, W., Ernst, J., Bilenky, M., Yen, A., Heravi-Moussavi, A., Kheradpour, P., Zhang, Z., Wang, J., Ziller, M.J., et al.; Roadmap Epigenomics Consortium (2015). Integrative analysis of 111 reference human epigenomes. *Nature* *518*, 317–330.
  23. Bernstein, B.E., Birney, E., Dunham, I., Green, E.D., Gunter, C., Snyder, M., and Consortium, E.P.; ENCODE Project Consortium (2012). An integrated encyclopedia of DNA elements in the human genome. *Nature* *489*, 57–74.
  24. Li, J., and Ji, L. (2005). Adjusting multiple testing in multilocus analyses using the eigenvalues of a correlation matrix. *Heredity (Edinb)* *95*, 221–227.
  25. Yang, J., Ferreira, T., Morris, A.P., Medland, S.E., Madden, P.A., Heath, A.C., Martin, N.G., Montgomery, G.W., Weedon, M.N., Loos, R.J., et al.; Genetic Investigation of ANthropometric Traits (GIANT) Consortium; DIABetes Genetics Replication And Meta-analysis (DIAGRAM) Consortium (2012). Conditional and joint multiple-SNP analysis of GWAS summary statistics identifies additional variants influencing complex traits. *Nat. Genet.* *44*, 369–375, S1–S3.
  26. Wright, S. (1965). The interpretation of population structure by F-statistics with special regard to systems of mating. *Evolution* *19*, 395–420.
  27. Wright, S. (1978). *Evolution and the Genetics of Population, Variability Within and Among Natural Populations* (University of Chicago Press).
  28. Balloux, F., and Lugon-Moulin, N. (2002). The estimation of population differentiation with microsatellite markers. *Mol. Ecol.* *11*, 155–165.
  29. Voight, B.F., Kudaravalli, S., Wen, X., and Pritchard, J.K. (2006). A map of recent positive selection in the human genome. *PLoS Biol.* *4*, e72.
  30. Kent, W.J., Sugnet, C.W., Furey, T.S., Roskin, K.M., Pringle, T.H., Zahler, A.M., and Haussler, D. (2002). The human genome browser at UCSC. *Genome Res.* *12*, 996–1006.
  31. Ng, M.C., Shriver, D., Chen, B.H., Li, J., Chen, W.M., Guo, X., Liu, J., Bielinski, S.J., Yanek, L.R., Nalls, M.A., et al.; FIND Consortium; eMERGE Consortium; DIAGRAM Consortium; MuTHER Consortium; MEta-analysis of type 2 Diabetes in African Americans Consortium (2014). Meta-analysis of genome-wide association studies in African Americans provides insights into the genetic architecture of type 2 diabetes. *PLoS Genet.* *10*, e1004517.
  32. Monda, K.L., Chen, G.K., Taylor, K.C., Palmer, C., Edwards, T.L., Lange, L.A., Ng, M.C., Adeyemo, A.A., Allison, M.A., Bielak, L.F., et al.; NABEC Consortium; UKBEC Consortium; BioBank Japan Project; AGEN Consortium (2013). A meta-analysis identifies new loci associated with body mass index in individuals of African ancestry. *Nat. Genet.* *45*, 690–696.
  33. Liu, C.T., Monda, K.L., Taylor, K.C., Lange, L., Demerath, E.W., Palmas, W., Wojczynski, M.K., Ellis, J.C., Vitolins, M.Z., Liu, S., et al. (2013). Genome-wide association of body fat distribution in African ancestry populations suggests new loci. *PLoS Genet.* *9*, e1003681.
  34. Franceschini, N., Fox, E., Zhang, Z., Edwards, T.L., Nalls, M.A., Sung, Y.J., Tayo, B.O., Sun, Y.V., Gottesman, O., Adeyemo, A., et al.; Asian Genetic Epidemiology Network Consortium (2013). Genome-wide association analysis of blood-pressure traits in African-ancestry individuals reveals common associated genes in African and non-African populations. *Am. J. Hum. Genet.* *93*, 545–554.
  35. Lettre, G., Palmer, C.D., Young, T., Ejebe, K.G., Allayee, H., Benjamin, E.J., Bennett, F., Bowden, D.W., Chakravarti, A., Dreisbach, A., et al. (2011). Genome-wide association study of coronary heart disease and its risk factors in 8,090 African Americans: the NHLBI CARE Project. *PLoS Genet.* *7*, e1001300.
  36. McCarty, C.A., Chisholm, R.L., Chute, C.G., Kullo, I.J., Jarvik, G.P., Larson, E.B., Li, R., Masys, D.R., Ritchie, M.D., Roden,

- D.M., et al.; eMERGE Team (2011). The eMERGE Network: a consortium of biorepositories linked to electronic medical records data for conducting genomic studies. *BMC Med. Genomics* 4, 13.
37. Gouda, H.N., Sagoo, G.S., Harding, A.H., Yates, J., Sandhu, M.S., and Higgins, J.P. (2010). The association between the peroxisome proliferator-activated receptor-gamma2 (PPARG2) Pro12Ala gene variant and type 2 diabetes mellitus: a HuGE review and meta-analysis. *Am. J. Epidemiol.* 171, 645–655.
  38. Gaulton, K.J., Nammo, T., Pasquali, L., Simon, J.M., Giresi, P.G., Fogarty, M.P., Panhuis, T.M., Mieczkowski, P., Secchi, A., Bosco, D., et al. (2010). A map of open chromatin in human pancreatic islets. *Nat. Genet.* 42, 255–259.
  39. Orho-Melander, M., Melander, O., Guiducci, C., Perez-Martinez, P., Corella, D., Roos, C., Tewhey, R., Rieder, M.J., Hall, J., Abecasis, G., et al. (2008). Common missense variant in the glucokinase regulatory protein gene is associated with increased plasma triglyceride and C-reactive protein but lower fasting glucose concentrations. *Diabetes* 57, 3112–3121.
  40. Beer, N.L., Tribble, N.D., McCulloch, L.J., Roos, C., Johnson, P.R., Orho-Melander, M., and Gloyn, A.L. (2009). The P446L variant in GCKR associated with fasting plasma glucose and triglyceride levels exerts its effect through increased glucokinase activity in liver. *Hum. Mol. Genet.* 18, 4081–4088.
  41. Jiang, W., Liu, Y., Liu, R., Zhang, K., and Zhang, Y. (2015). The lncRNA DEANR1 facilitates human endoderm differentiation by activating FOXA2 expression. *Cell Rep.* 11, 137–148.
  42. Ng, M.C., Saxena, R., Li, J., Palmer, N.D., Dimitrov, L., Xu, J., Rasmussen-Torvik, L.J., Zmuda, J.M., Siscovick, D.S., Patel, S.R., et al. (2013). Transferability and fine mapping of type 2 diabetes loci in African Americans: the Candidate Gene Association Resource Plus Study. *Diabetes* 62, 965–976.
  43. Schaub, M.A., Boyle, A.P., Kundaje, A., Batzoglou, S., and Snyder, M. (2012). Linking disease associations with regulatory information in the human genome. *Genome Res.* 22, 1748–1759.
  44. Maurano, M.T., Humbert, R., Rynes, E., Thurman, R.E., Haugen, E., Wang, H., Reynolds, A.P., Sandstrom, R., Qu, H., Brody, J., et al. (2012). Systematic localization of common disease-associated variation in regulatory DNA. *Science* 337, 1190–1195.
  45. Claussnitzer, M., Dankel, S.N., Klocke, B., Grallert, H., Glunk, V., Berulava, T., Lee, H., Oskolkov, N., Fadista, J., Ehlers, K., et al.; DIAGRAM+Consortium (2014). Leveraging cross-species transcription factor binding site patterns: from diabetes risk loci to disease mechanisms. *Cell* 156, 343–358.
  46. Matthews, D.R., Hosker, J.P., Rudenski, A.S., Naylor, B.A., Treacher, D.F., and Turner, R.C. (1985). Homeostasis model assessment: insulin resistance and beta-cell function from fasting plasma glucose and insulin concentrations in man. *Diabetologia* 28, 412–419.
  47. Laakso, M. (1993). How good a marker is insulin level for insulin resistance? *Am. J. Epidemiol.* 137, 959–965.
  48. Kahn, S.E., Prigeon, R.L., McCulloch, D.K., Boyko, E.J., Bergman, R.N., Schwartz, M.W., Neifing, J.L., Ward, W.K., Beard, J.C., Palmer, J.P., et al. (1993). Quantification of the relationship between insulin sensitivity and beta-cell function in human subjects. Evidence for a hyperbolic function. *Diabetes* 42, 1663–1672.
  49. Weyer, C., Hanson, R.L., Tataranni, P.A., Bogardus, C., and Pratley, R.E. (2000). A high fasting plasma insulin concentration predicts type 2 diabetes independent of insulin resistance: evidence for a pathogenic role of relative hyperinsulinemia. *Diabetes* 49, 2094–2101.
  50. Ferrannini, E., Natali, A., Bell, P., Cavallo-Perin, P., Lalic, N., and Mingrone, G.; European Group for the Study of Insulin Resistance (EGIR) (1997). Insulin resistance and hypersecretion in obesity. *J. Clin. Invest.* 100, 1166–1173.
  51. Corkey, B.E. (2012). Banting lecture 2011: hyperinsulinemia: cause or consequence? *Diabetes* 61, 4–13.
  52. Corkey, B.E. (2012). Diabetes: have we got it all wrong? Insulin hypersecretion and food additives: cause of obesity and diabetes? *Diabetes Care* 35, 2432–2437.
  53. Chen, C.H., Cruz, L.A., and Mochly-Rosen, D. (2015). Pharmacological recruitment of aldehyde dehydrogenase 3A1 (ALDH3A1) to assist ALDH2 in acetaldehyde and ethanol metabolism in vivo. *Proc. Natl. Acad. Sci. USA* 112, 3074–3079.
  54. Doudna, J.A., and Charpentier, E. (2014). Genome editing. The new frontier of genome engineering with CRISPR-Cas9. *Science* 346, 1258096.
  55. Pautsch, A., Stadler, N., Löhle, A., Rist, W., Berg, A., Glocker, L., Nar, H., Reinert, D., Lenter, M., Heckel, A., et al. (2013). Crystal structure of glucokinase regulatory protein. *Biochemistry* 52, 3523–3531.
  56. Saxena, R., Voight, B.F., Lyssenko, V., Burt, N.P., de Bakker, P.I., Chen, H., Roix, J.J., Kathiresan, S., Hirschhorn, J.N., Daly, M.J., et al.; Diabetes Genetics Initiative of Broad Institute of Harvard and MIT, Lund University, and Novartis Institutes of BioMedical Research (2007). Genome-wide association analysis identifies loci for type 2 diabetes and triglyceride levels. *Science* 316, 1331–1336.
  57. Vaxillaire, M., Cavalcanti-Proença, C., Dechaume, A., Tichet, J., Marre, M., Balkau, B., and Froguel, P.; DESIR Study Group (2008). The common P446L polymorphism in GCKR inversely modulates fasting glucose and triglyceride levels and reduces type 2 diabetes risk in the DESIR prospective general French population. *Diabetes* 57, 2253–2257.
  58. Udler, M.S., Ahmed, S., Healey, C.S., Meyer, K., Struwing, J., Maranian, M., Kwon, E.M., Zhang, J., Tyrer, J., Karlins, E., et al. (2010). Fine scale mapping of the breast cancer 16q12 locus. *Hum. Mol. Genet.* 19, 2507–2515.
  59. Franceschini, N., van Rooij, F.J., Prins, B.P., Feitosa, M.F., Karakas, M., Eckfeldt, J.H., Folsom, A.R., Kopp, J., Vaez, A., Andrews, J.S., et al.; LifeLines Cohort Study (2012). Discovery and fine mapping of serum protein loci through transethnic meta-analysis. *Am. J. Hum. Genet.* 91, 744–753.
  60. Liu, C.T., Buchkovich, M.L., Winkler, T.W., Heid, I.M., Borecki, I.B., Fox, C.S., Mohlke, K.L., North, K.E., Adrienne Cupples, L., Consortium, A.A.A.G., et al.; African Ancestry Anthropometry Genetics Consortium; GIANT Consortium (2014). Multi-ethnic fine-mapping of 14 central adiposity loci. *Hum. Mol. Genet.* 23, 4738–4744.
  61. Ong, R.T., and Teo, Y.Y. (2010). varLD: a program for quantifying variation in linkage disequilibrium patterns between populations. *Bioinformatics* 26, 1269–1270.